Studies of low-energy K- nucleus/nuclei interactions by AMADEUS

Magdalena Skurzok

On the behalf of the AMADEUS collaboration

Jagiellonian University in Krakow

Istituto Nazionale di Fisica Nucleare

LNF

NSTAR2022 Conference

Santa Margherita Ligure, 17-21.10.2022

Motivation and Scientific Case

The investigation of the **in-medium modification of the $\bar{K}N$ interaction** is of **fundamental** for the low-energy QCD (Quantum Chromodynamic)

Chiral perturbation theory (ChPT): effective field theory where **mesons and baryons** represent the effective degrees of freedom instead of the fundamental quark and gluon fields.

$$\mathcal{L}_{eff} = \mathcal{L}_{mesons}(\Phi) + \mathcal{L}_B(\Phi, \Psi_B)$$

- The chiral symmetry is **spontaneously broken** → the existence of massless and spinless Nambu-Goldstone bosons which are identified with the pions. Explicitly broken by **q** masses.
- **Very successful** in describing the πN, ππ and NN interactions in the low-energy regime and is considered as the theory of the low-energy strong interaction **in the SU(2) flavour sector**.

The extension of the theory to the sector with the quark s turns out to be more problematic since it is not directly applicable to the $\bar{K}N$ channel.

The χPT is not applicable to the $\bar{K}N$ channel due to the emerging of the Λ(1405) and the Σ(1385) resonances just below the $\bar{K}N$ mass threshold

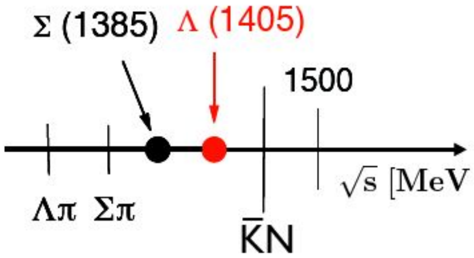

Λ(1405) I=0 $J^P = ½^-$

M = $(1405.1^{+1.3}_{-1.0})$ MeV Γ = (50.5 ± 2.0) MeV

decay modes: Σπ (I=0) 100%

Σ(1385) I=1 $J^P = 3/2^+$

decay modes: Λ π (I=1) (87.0 ± 1.5) %

Σ π (I=1) (11.7 ± 1.5) %

Possible solutions:

- **Non-perturbative Coupled Channels approach: Chiral Unitary SU(3) Dynamics**
- **Phenomenological $\bar{K}N$ and NN potentials**

The χPT is not applicable to the $\bar{K}N$ channel due to the emerging of the Λ(1405) and the Σ(1385) resonances just below the $\bar{K}N$ mass threshold

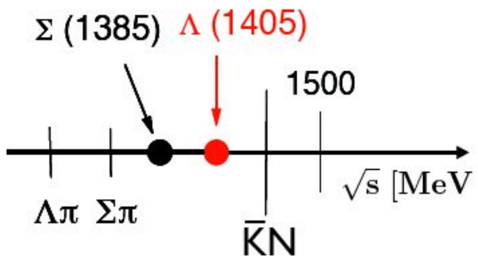

Λ(1405) I=0 $J^P = ½^-$

M = $(1405.1^{+1.3}_{-1.0})$ MeV Γ = (50.5 ± 2.0) MeV

decay modes: Σπ (I=0) 100%

Σ(1385) I=1 $J^P = 3/2^+$

decay modes: Λ π (I=1) (87.0 ± 1.5) %

Σ π (I=1) (11.7 ± 1.5) %

Possible solutions:

- ➢ **Non-perturbative Coupled Channels approach: Chiral Unitary SU(3) Dynamics**
- ➢ **Phenomenological $\bar{K}N$ and NN potentials**

The parameters of the models are constrained by the existing scattering data

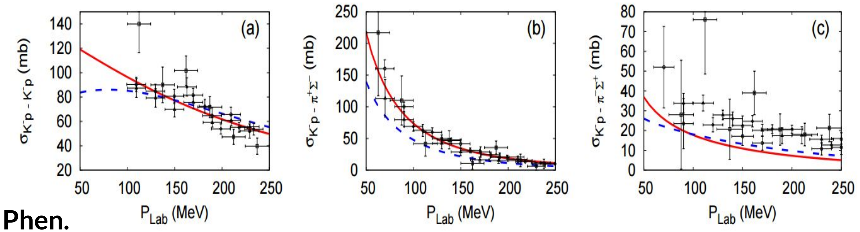

Phen.

Y. Ikeda and T. Sato, Phys. Rev. C76, 035203 (2007)

Chiral

S. Ohnishi, Y. Ikeda, T. Hyodo, W. Weise, Phys.Rev. C93 (2016) no.2, 025207

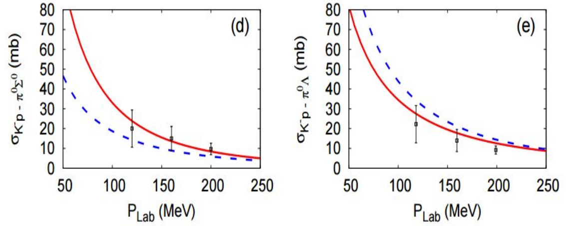

...but... large differences in the subthreshold extrapolations!

Significantly weaker attraction in chiral SU(3) models than in phenomenological potential models.

Re	Im		
———	- - - -	**Phen.**	[Y. Akaishi, T. Yamazaki, Phys. Rev. C65, 044005 (2002)]
▬▬	▬ ▬	**Chiral**	[Y. Ikeda, T. Hyodo, W. Weise, Phys. Lett. B706, 63 (2011)]

Phenomenologic potential model

Chiral SU(3) dynamics

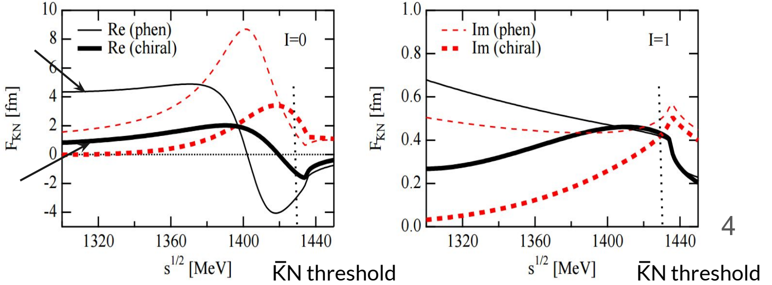

The controversial nature of the **Λ(1405) and kaonic bound states**

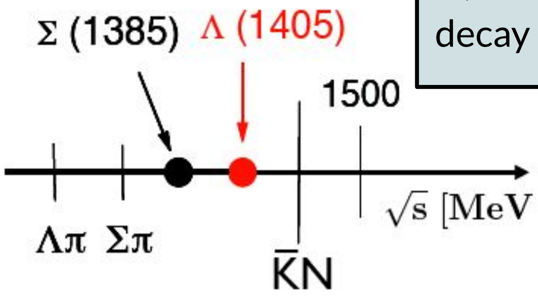

Λ(1405) I=0 $J^P = ½^-$
decay modes: Σπ (I=0)

The Λ(1405) state does not fit with the simple three quarks model (*uds*) and it is commonly accepted that **it is, at least partially, a $\bar{K}N$ bound state.**

Wycech (1986) - Akaishi & Yamazaki (2002)

Predicted in the **KN interaction in the I=0** channel due to the strong interaction

Essential impact on the EoS of Neutron Stars

gravitational waves signal emitted by binary system of Neutron Stars

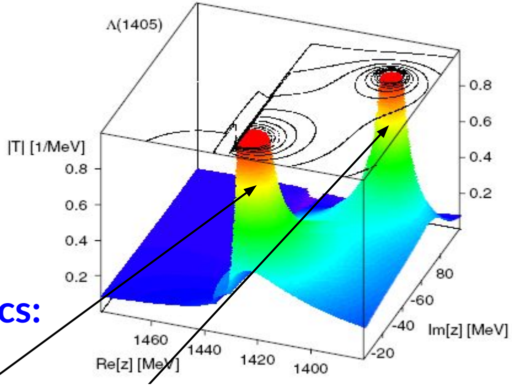

- **Chiral SU(3) coupled channel dynamics:**
  the state is given by the superpositions of **two poles of the $\bar{K}N$ scattering amplitude**.

  M = 1425 MeV → **mainly coupled to the $\bar{K}N$ channel**

  M = 1380 MeV → **mainly coupled to the Σπ channel**

- **Phenomenological potentials models:**
  the **Λ(1405) is a pure $\bar{K}N$ bound state** with mass M=1405 MeV, binding energy BE = 27 MeV and width Γ=50 MeV.

E15 → first clear evidence in K^- induced reactions
Phys.Lett.B 789 (2019) 620-625

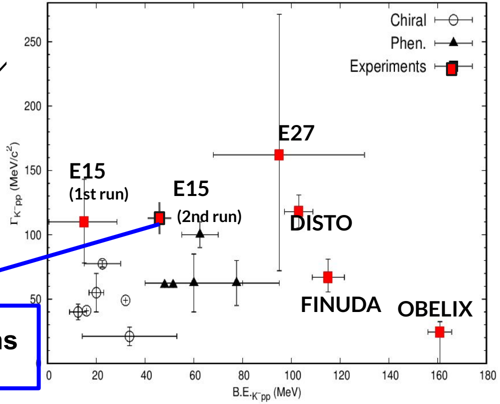

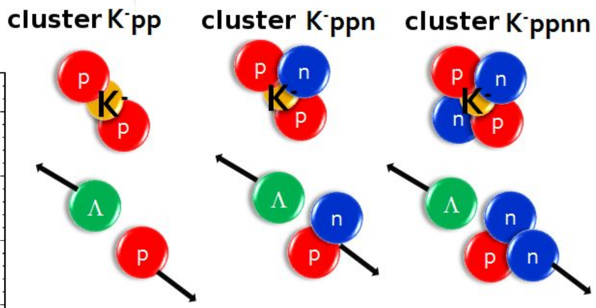

Λ + p Σ^0 + p	Λ + d Σ^0 + d	Λ + t Σ^0 + t

AMADEUS @ DAΦNE

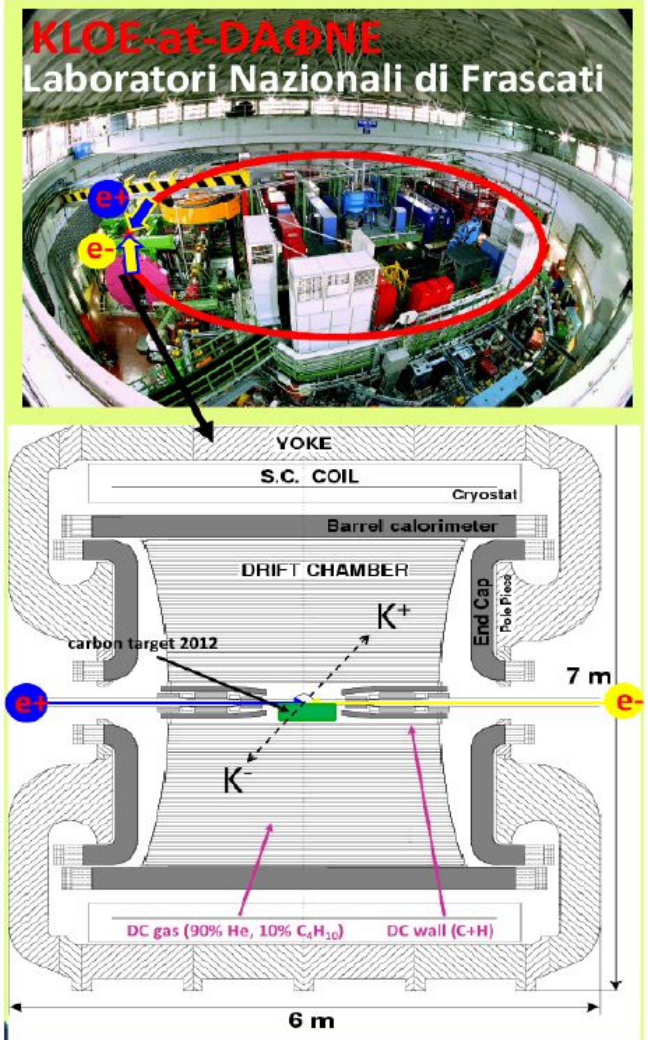

DAΦNE

- $\phi \rightarrow K^- K^+$ (49.2%), ≈1000 ϕ/s
- monochromatic **low momentum** Kaons ≈127 Mev/c
- **back to back** $K^- K^+$ topology
- **small hadronic background** due to the beam

KLOE

- Cilindrical DC with **4π geometry** & electromagnetic calormeter
- **96% acceptance**
- **high efficiency and resolution** for charged and neutral particles
- exclusive measurement of the considered

AT-REST
K^- absorbed from atomic orbitals
(p_K ~ 0 MeV/c)

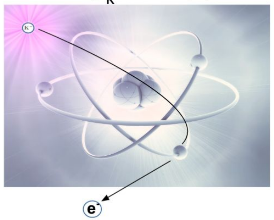

IN-FLIGHT
(p_K~ 100 MeV/c)

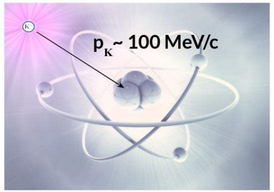

AMADEUS: KLOE 2004-2005 dataset analysis ($\mathcal{L}$ = 1.74 pb-1)

Possibility to use **KLOE materials** as an **active target**

- DC wall (750 μm C foil , 150 μm Al foil);
- DC gas (90% He, 10% C_4H_{10}).

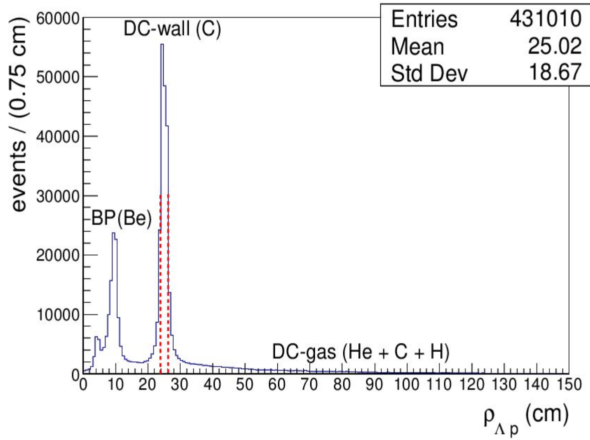

AMADEUS @ DAΦNE

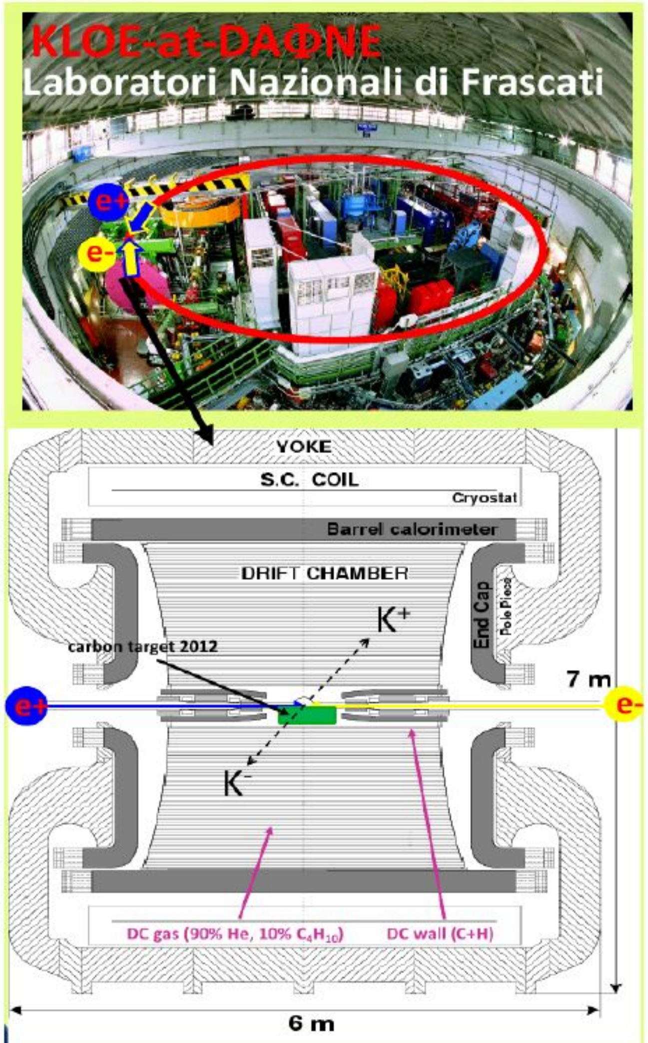

DAΦNE

- $\phi \rightarrow K^- K^+$ (49.2%), ≈1000 ϕ/s
- monochromatic **low momentum** Kaons ≈127 Mev/c
- **back to back** $K^- K^+$ topology
- **small hadronic background** due to the beam

KLOE

- Cilindrical DC with **4π geometry** & electromagnetic calormeter
- **96% acceptance**
- **high efficiency and resolution** for charged and neutral particles
- exclusive measurement of the considered

K^- absorption on light nuclei AT REST & IN FLIGHT

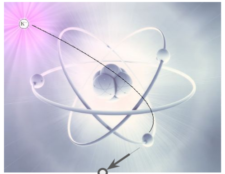

K- absorbed from atomic orbit

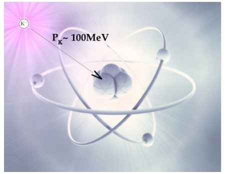

AMADEUS: KLOE 2004-2005 dataset analysis ($\mathcal{L}$ = 1.74 pb-1)

AMADEUS scientific case

- nature of Λ(1405) and K^-N amplitude below threshold

- low-energy charged K cross section (for p=100MeV)

⇓

Yπ correlation studies (Λπ, Σπ final states)

- K^- multiN absorption

- kaonic nuclear clusters

⇓

YN correlation studies (Λp, $\Sigma^0 p$, Λt final states)

$\Lambda\pi^-$ analysis: K^-n non-resonant transition amplitude

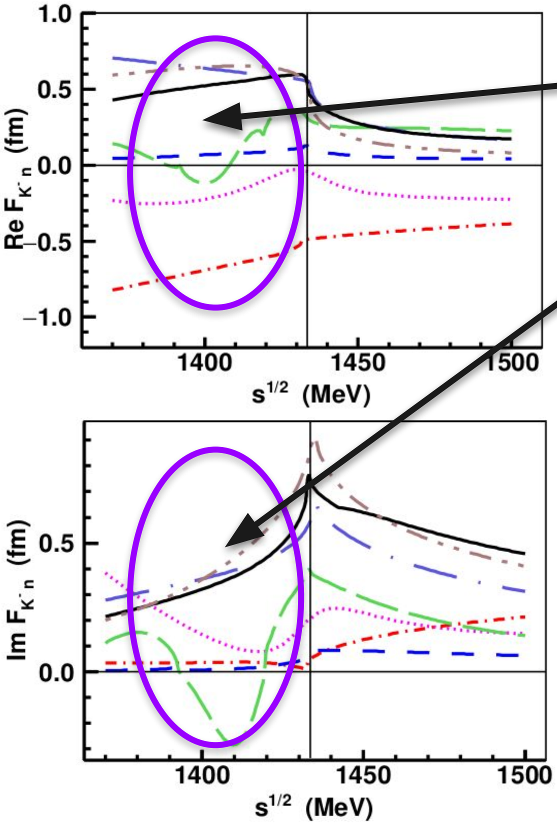

First determination of the non-resonant transition amplitude below threshold

Investigated using:

K^-"n" → $\Lambda\pi^-$ direct formation in ^{4}**He** (DC volume)

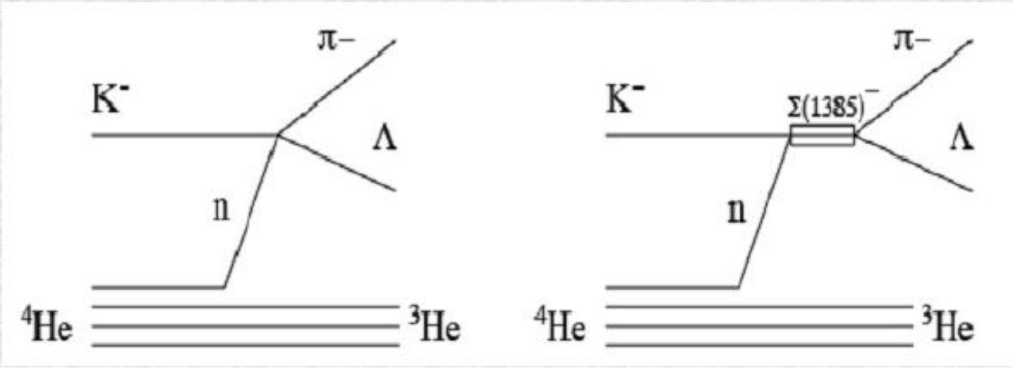

$$|f^{N\text{-}R}_{\Lambda\pi}(I=1)| \Rightarrow |f^{N\text{-}R}_{\Sigma\pi}(I=0)|$$

K^-n scattering amplitude with Chiral models

J. Hrtankova, J. Mares, Phys. Rev. C96, 015205 (2017)
A. Cieply et al, Nycl. Phys. A 954, 17 (2016)

The detailed characterisation of the yield and spectral shape of the non-resonant antiKN absorption is fundamental reference to extract the Λ(1405) properties in $\bar{K}$N absorption experiments

non-resonant transition amplitude below threshold

Channels	Ratio/yield	σ_{stat}	σ_{syst}
RES-ar/NR-ar	0.39	± 0.04	$^{+0.18}_{-0.07}$
RES-if/NR-if	0.23	± 0.03	$^{+0.23}_{-0.22}$
NR-ar	12.0%	± 1.7%	$^{+2.0}_{-2.8}$%
NR-if	19.2%	± 4.4%	$^{+5.9}_{-3.3}$%
$\Sigma \to \Lambda$ conv.	2.2%	± 0.3%	$^{+1.6}_{-0.8}$%
$K^{-12}C$ capture	57.0%	± 1.2%	$^{+2.2}_{-3.2}$%

Simultaneous fit : ($p_{\Lambda\pi-}$ - $m_{\Lambda\pi-}$ - $\cos(\theta_{\Lambda\pi-})$

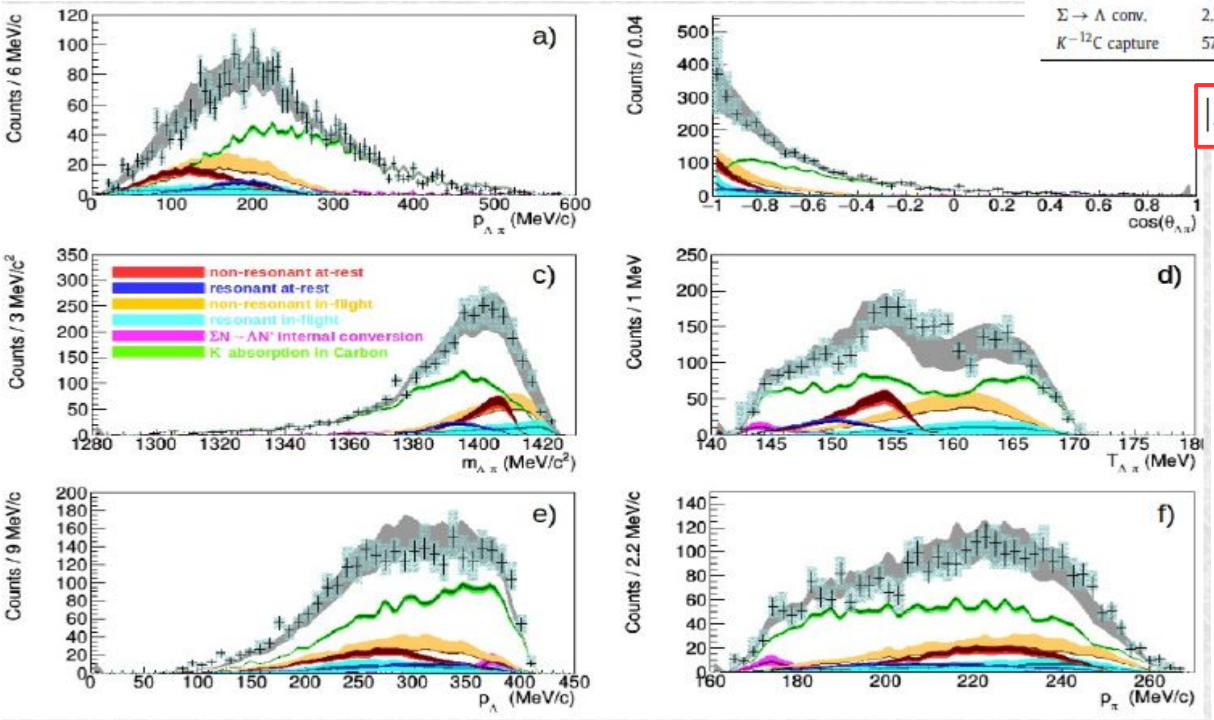

$$|A_{K^- n \to \Lambda\pi^-}| = (0.334 \pm 0.018\,\mathrm{stat}^{+0.034}_{-0.058}\,\mathrm{syst})\ \mathrm{fm}$$

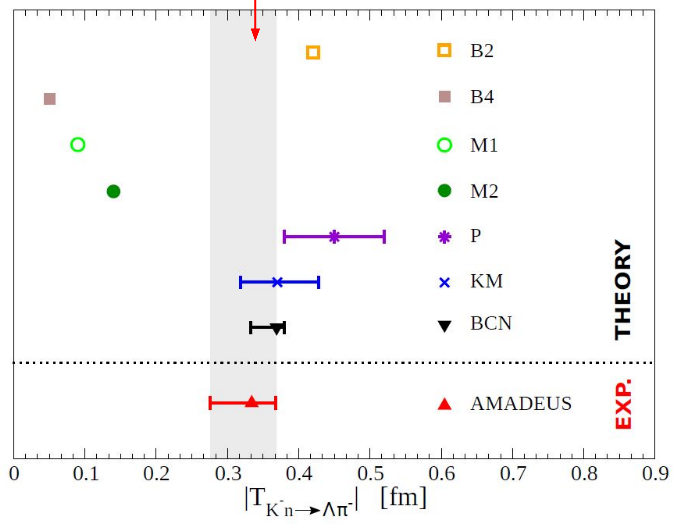

Investigated using: **K⁻ “n”** ^{3}He → **Λπ⁻** ^{3}He

$$E_{Kn} \sim -B_n - < \frac{p^2_{\Lambda\pi}}{2\mu_{\pi,\Lambda,3He}} >$$ (33±6) MeV below KN threshold

K. Piscicchia, et. al., Phys. Lett. B782, 339 (2018)
K. Piscicchia, S. Wycech, C. Curceanu, Nucl. Phys. A 954, 75 (2016)

$\Sigma^0\pi^0/\Lambda^0\pi^0$ analysis

Motivation:

1) The available data for the inelastic $K^- p \to \Sigma^0 \pi^0$ cross section close to threshold:

- three points in the p_K=120-200 MeV/c range (bubble chamber experiments),
- uncertainties larger than 30%,
- the $K^- p \to \Sigma^0 \pi^0$ cross sections are obtained **not directly but** on the basis of the isospin symmetry argument, from the measurement of $K^- p \to \Lambda\pi^0$ events

Low momentum K^- scattering cross sections in this Isospin I = 0 channel represent a fundamental input for the non-perturbative low energy QCD models

[1] W. E. Humphrey and R. R. Ross, Phys. Rev. 127 (1962) 1305.
[2] J. K. Kim, Columbia University Report No. NEVIS-149 (1966).

Theoretical calculation:
Y. Ikeda, T. Hyodo, W. Weise, Nucl. Phys. A 881 (2012) 98.

no experimental data

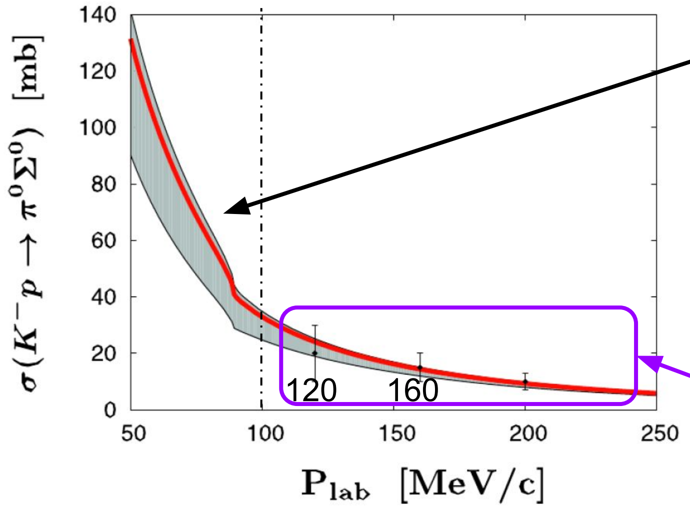

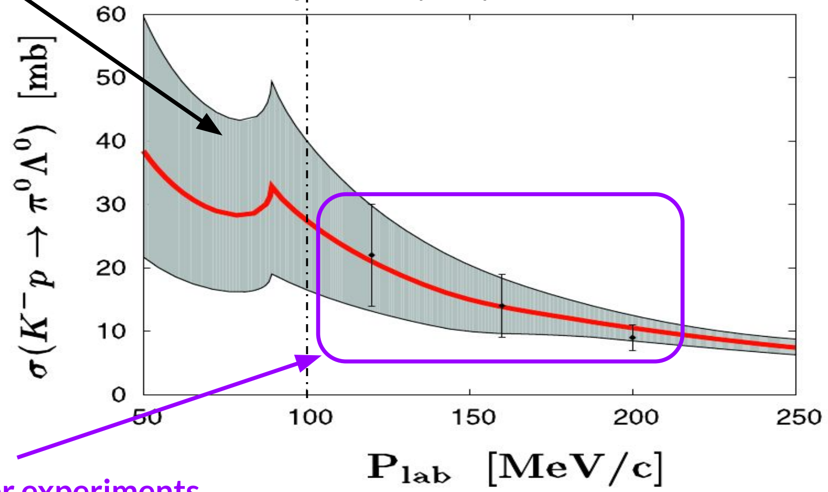

bubble chamber experiments

$\Sigma^0\pi^0/\Lambda^0\pi^0$ analysis

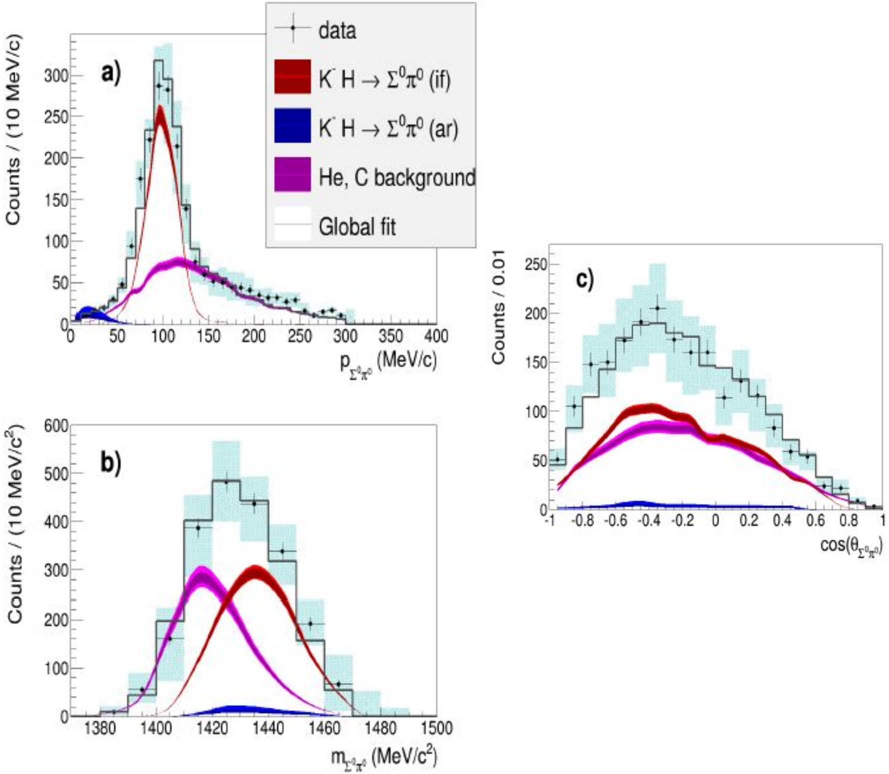

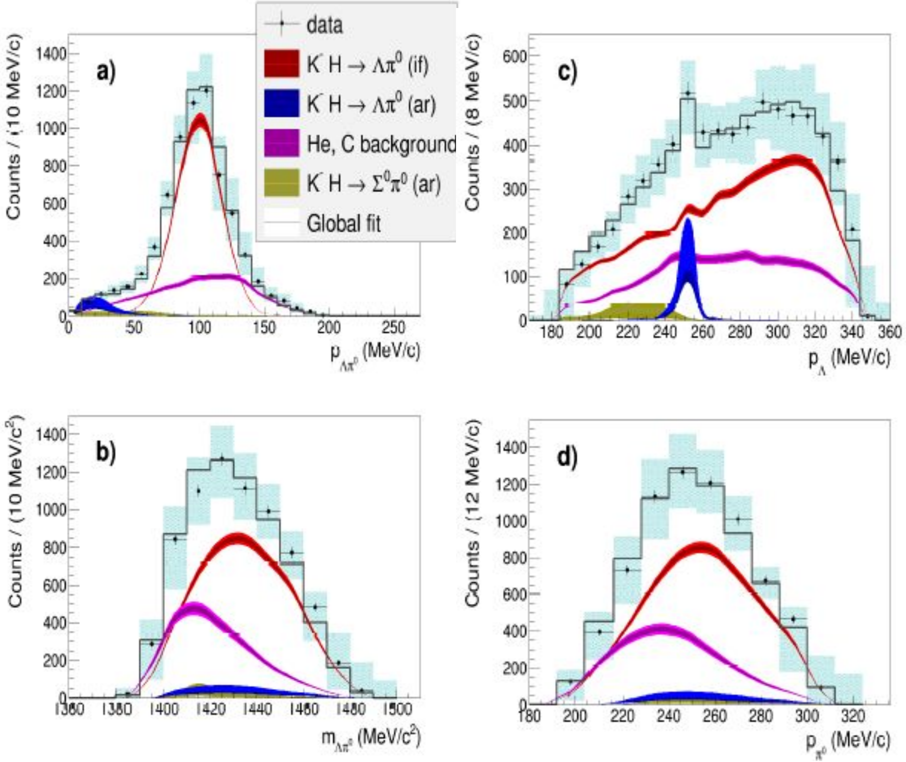

PRELIMINARY

$\Sigma^0\pi^0/\Lambda^0\pi^0$ analysis

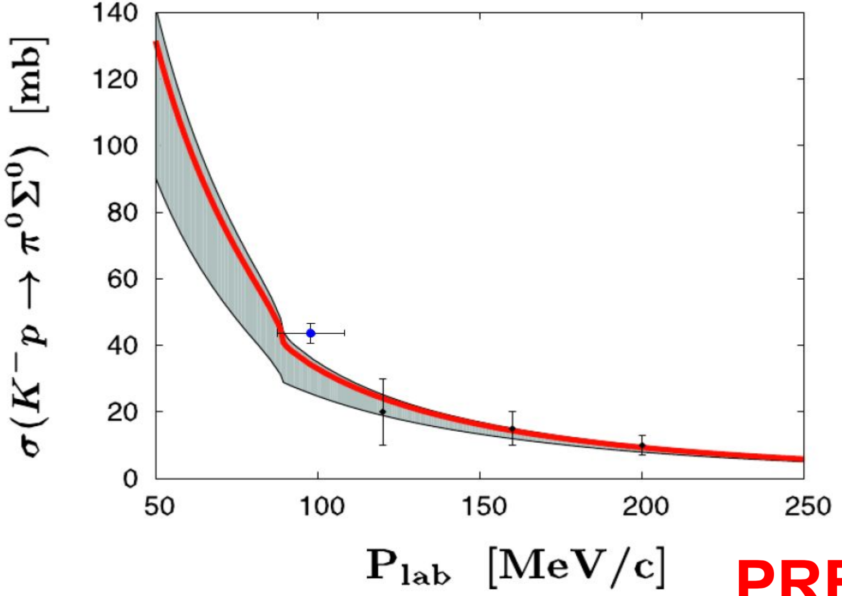

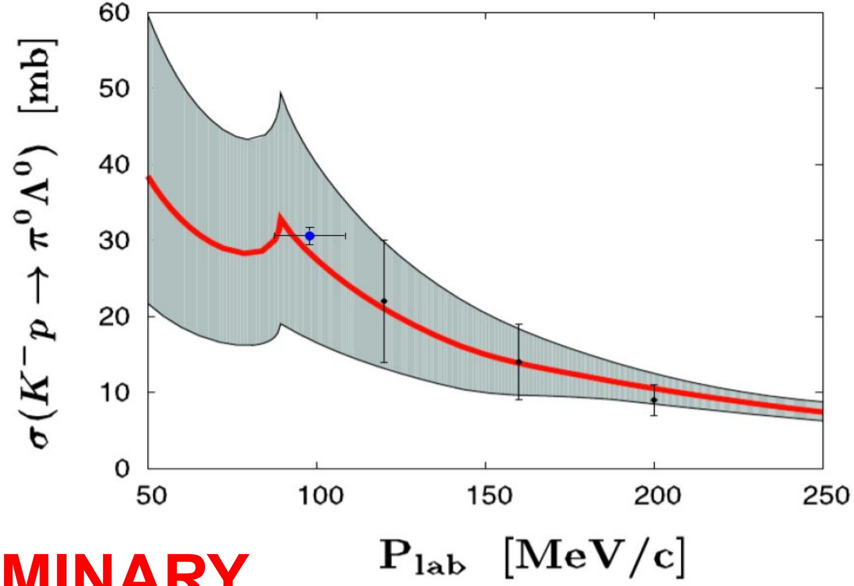

PRELIMINARY

$\sigma(K^- p \to \Sigma^0\pi^0)(p_K = (98 \pm 10)MeV/c) = 42.8 \pm 1.5(stat.)^{+2.4}_{-2.0}(syst.)$ mb

$\sigma(K^- p \to \Lambda\pi^0)(p_K = (98 \pm 10)MeV/c) = 31.0 \pm 0.5(stat.)^{+1.2}_{-1.2}(syst.)$ mb

K^- multi-nucleon absorptions

In K^--nuclei optical potential a K^- multi-nucleon absorption term is necessary to fit the kaonic atoms data:

$$V_{K-}(\rho) = V_{K-}^{(1)}(\rho) + V_{K-}^{(2)}(\rho) \rightarrow$$ **multi-nucleon term**

[E. Friedman, A. Gal, Nucl. Phys. A 959, 66 (2017)]
[Hrtánková, J. & Mareš, J. Phys. Rev. C96, 015205 (2017)]

single nucleon term from chiral models

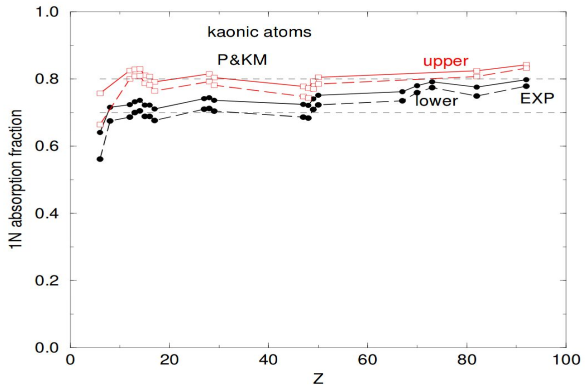

- **Single nucleon absorption (1NA):** K^- "N" $\rightarrow Y\pi$ ⟶ pionic processes
- **Two nucleon absorption (2NA):** K^- "NN" $\rightarrow$ Y N
- **Three nucleon absorption (3NA):** K^- "NNN" $\rightarrow$ Y (NN) ⟶ non-pionic processes
- **Four nucleon absorption (4NA):** K^- "NNNN" $\rightarrow$ Y (NNN)

bound nucleons = "N", "NN", "NNN", "NNNN"
bound or unbound nucleons = (NN), (NNN)
Y = Λ, Σ

Λp analysis: K^- multi-nucleon absorption BRs and σ

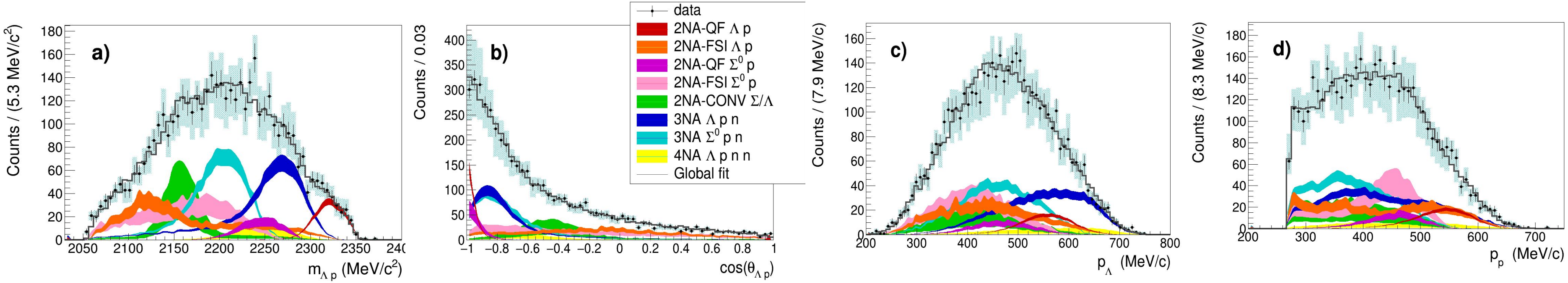

R. Del Grande et al., Eur .Phys. J. C 79 (2019) no. 3, 190

Simultaneous fit of:

- Λp invariant mass;
- angular correlation;
- proton momentum;
- Λ momentum.

Process	Branching Ratio (%)	σ (mb)	@	p_K (MeV/c)
2NA-QF Λp	0.25 ± 0.02 (stat.) $^{+0.01}_{-0.02}$(syst.)	2.8 ± 0.3 (stat.) $^{+0.1}_{-0.2}$ (syst.)	@	128 ± 29
2NA-FSI Λp	6.2 ± 1.4(stat.) $^{+0.5}_{-0.6}$(syst.)	69 ± 15 (stat.) ± 6 (syst.)	@	128 ± 29
2NA-QF Σ^0p	0.35 ± 0.09(stat.) $^{+0.13}_{-0.06}$(syst.)	3.9 ± 1.0 (stat.) $^{+1.4}_{-0.7}$ (syst.)	@	128 ± 29
2NA-FSI Σ^0p	7.2 ± 2.2(stat.) $^{+4.2}_{-5.4}$(syst.)	80 ± 25 (stat.) $^{+46}_{-60}$ (syst.)	@	128 ± 29
2NA-CONV Σ/Λ	2.1 ± 1.2(stat.) $^{+0.9}_{-0.5}$(syst.)	-		
3NA Λpn	1.4 ± 0.2(stat.) $^{+0.1}_{-0.2}$(syst.)	15 ± 2 (stat.) ± 2 (syst.)	@	117 ± 23
3NA Σ^0pn	3.7 ± 0.4(stat.) $^{+0.2}_{-0.4}$(syst.)	41 ± 4 (stat.) $^{+2}_{-5}$ (syst.)	@	117 ± 23
4NA Λpnn	0.13 ± 0.09(stat.) $^{+0.08}_{-0.07}$(syst.)	-		
Global $\Lambda(\Sigma^0)$p	21 ± 3(stat.) $^{+5}_{-6}$(syst.)	-		

cross sections and BRs

Λp analysis: K^- multi-nucleon absorption BRs and σ

Process	Branching Ratio (%)	σ (mb)	@	p_K (MeV/c)
2NA-QF Λp	0.25 ± 0.02 (stat.) $^{+0.01}_{-0.02}$(syst.)	2.8 ± 0.3 (stat.) $^{+0.1}_{-0.2}$ (syst.)	@	128 ± 29
2NA-FSI Λp	6.2 ± 1.4(stat.) $^{+0.5}_{-0.6}$(syst.)	69 ± 15 (stat.) $\pm$ 6 (syst.)	@	128 ± 29
2NA-QF $\Sigma^0 p$	0.35 ± 0.09(stat.) $^{+0.13}_{-0.06}$(syst.)	3.9 ± 1.0 (stat.) $^{+1.4}_{-0.7}$ (syst.)	@	128 ± 29
2NA-FSI $\Sigma^0 p$	7.2 ± 2.2(stat.) $^{+4.2}_{-5.4}$(syst.)	80 ± 25 (stat.) $^{+46}_{-60}$ (syst.)	@	128 ± 29
2NA-CONV Σ/Λ	2.1 ± 1.2(stat.) $^{+0.9}_{-0.5}$(syst.)	-		
3NA Λpn	1.4 ± 0.2(stat.) $^{+0.1}_{-0.2}$(syst.)	15 ± 2 (stat.) $\pm$ 2 (syst.)	@	117 ± 23
3NA $\Sigma^0 pn$	3.7 ± 0.4(stat.) $^{+0.2}_{-0.4}$(syst.)	41 ± 4 (stat.) $^{+2}_{-5}$ (syst.)	@	117 ± 23
4NA Λpnn	0.13 ± 0.09(stat.) $^{+0.08}_{-0.07}$(syst.)	-		
Global $\Lambda(\Sigma^0)p$	21 ± 3(stat.) $^{+5}_{-6}$(syst.)	-		

R. Del Grande et al., Eur. Phys. J. C79 (2019) no.3, 190

The ratio between the branching ratios of the 2NA-QF in the Λp channel and in the Σ^0p is measured to be:

$$\mathcal{R} = \frac{BR(K^- pp \to \Lambda p)}{BR(K^- pp \to \Sigma^0 p)} = 0.7 \pm 0.2(stat.)^{+0.2}_{-0.3}(syst.)$$

and the ratio between the corresponding phase spaces is $\mathcal{R}' \simeq 1.22$.

Information on the in-medium dynamics

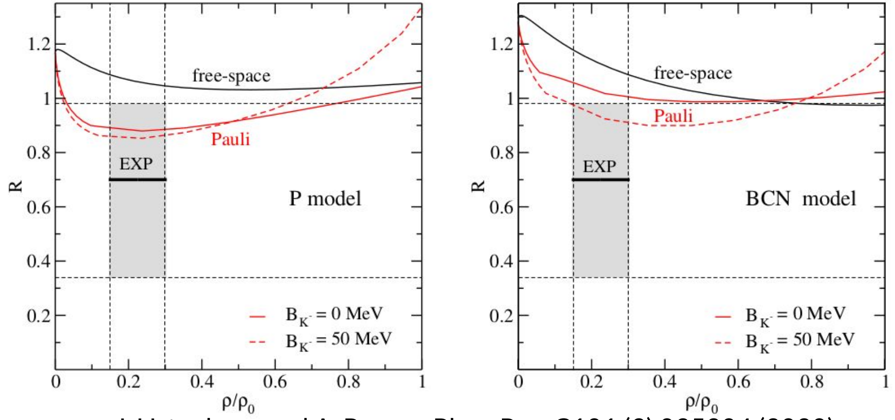

J. Hrtankova and A. Ramos, Phys. Rev. C101 (3) 035204 (2020)

Λp analysis: K⁻pp bound state search

Using BE and Γ from experiments:

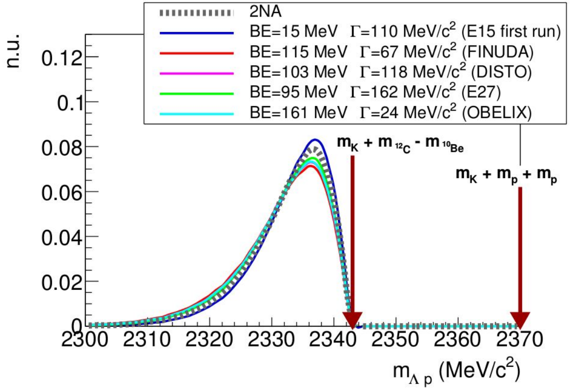

Fixing BE and moving Γ:

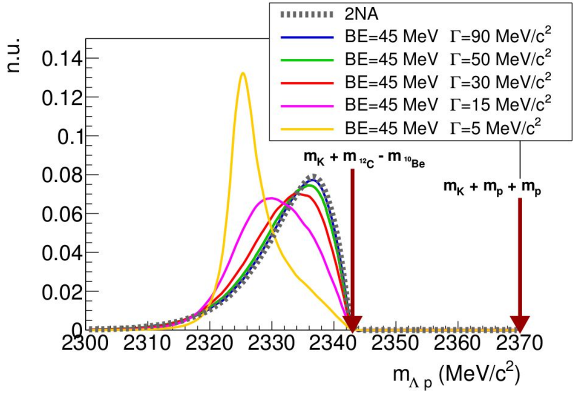

AMADEUS at DAΦNE

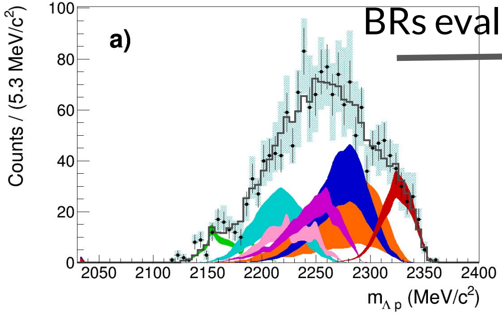

BRs evaluation

R. Del Grande et al., Eur.Phys.J. C79 (2019) no.3, 190

Process	Branching Ratio (%)
2NA-QF Λp	$0.20 \pm 0.04(\text{stat.}) \pm 0.02(\text{syst.})$
2NA-FSI Λp	$3.8 \pm 2.3(\text{stat.}) \pm 1.1(\text{syst.})$
2NA-QF Σ^0p	$0.54 \pm 0.20(\text{stat.})\ ^{+0.20}_{-0.16}(\text{syst.})$
2NA-FSI Σ^0p	$5.4 \pm 1.5(\text{stat.})\ ^{+1.0}_{-2.7}(\text{syst.})$
2NA-CONV Σ/Λ	$22 \pm 4(\text{stat.})\ ^{+1}_{-12}(\text{syst.})$
3NA Λpn	$1.1 \pm 0.3(\text{stat.}) \pm 0.2(\text{syst.})$
3NA Σ^0pn	$1.9 \pm 0.7(\text{stat.})\ ^{+0.8}_{-0.4}(\text{syst.})$

FINUDA at DAΦNE

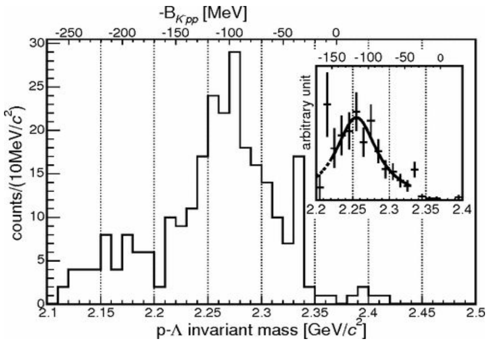

[M. Agnello et al., Phys. Rev. Lett. 94, 212303 (2005)]

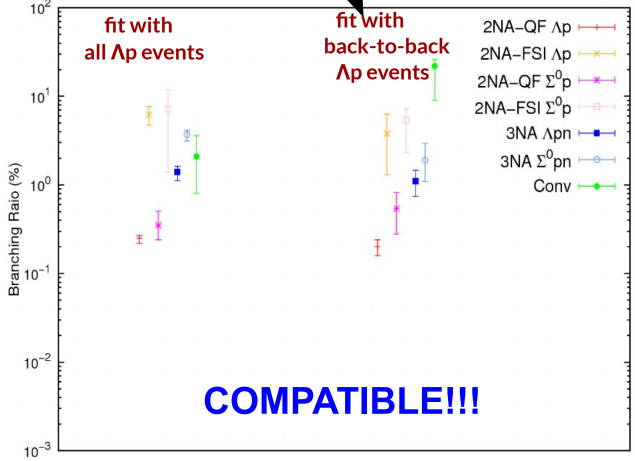

K⁻pp bound state contribution **completely overlaps** with the K⁻2NA

Summary

K^-n amplitude below threshold

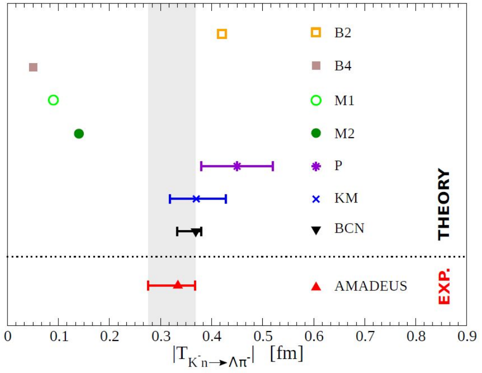

Λ p channel: 2NA, 3NA and 4NA BRs and σ

Process	Branching Ratio (%)	σ (mb)	@	p_K (MeV/c)
2NA-QF Λp	0.25 ± 0.02 (stat.) $^{+0.01}_{-0.02}$(syst.)	2.8 ± 0.3 (stat.) $^{+0.1}_{-0.2}$ (syst.)	@	128 ± 29
2NA-FSI Λp	6.2 ± 1.4(stat.) $^{+0.5}_{-0.6}$(syst.)	69 ± 15 (stat.) ± 6 (syst.)	@	128 ± 29
2NA-QF $\Sigma^0 p$	0.35 ± 0.09(stat.) $^{+0.13}_{-0.06}$(syst.)	3.9 ± 1.0 (stat.) $^{+1.4}_{-0.7}$ (syst.)	@	128 ± 29
2NA-FSI $\Sigma^0 p$	7.2 ± 2.2(stat.) $^{+4.2}_{-5.4}$(syst.)	80 ± 25 (stat.) $^{+46}_{-60}$ (syst.)	@	128 ± 29
2NA-CONV Σ/Λ	2.1 ± 1.2(stat.) $^{+0.9}_{-0.5}$(syst.)	-		
3NA Λpn	1.4 ± 0.2(stat.) $^{+0.1}_{-0.2}$(syst.)	15 ± 2 (stat.) ± 2 (syst.)	@	117 ± 23
3NA $\Sigma^0 pn$	3.7 ± 0.4(stat.) $^{+0.2}_{-0.4}$(syst.)	41 ± 4 (stat.) $^{+2}_{-5}$ (syst.)	@	117 ± 23
4NA Λpnn	0.13 ± 0.09(stat.) $^{+0.08}_{-0.07}$(syst.)	-		
Global $\Lambda(\Sigma^0)p$	21 ± 3(stat.) $^{+5}_{-6}$(syst.)	-		

$K^-p \to \Sigma^0\pi^0/\Lambda\pi^0$ cross sections

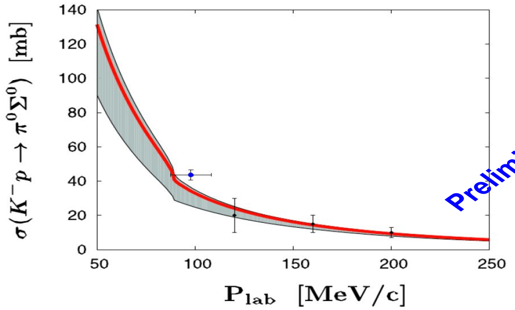

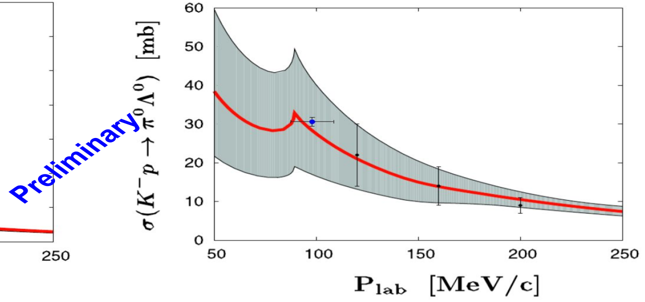

$\sigma(K^-p \to \Sigma^0\pi^0)(p_K = (98 \pm 10)MeV/c) = 42.8 \pm 1.5(stat.)^{+2.4}_{-2.0}(syst.)$ mb

$\sigma(K^-p \to \Lambda\pi^0)(p_K = (98 \pm 10)MeV/c) = 31.0 \pm 0.5(stat.)^{+1.2}_{-1.2}(syst.)$ mb

Thank you for attention!

Experimental constraints above threshold

K^-p scattering amplitude

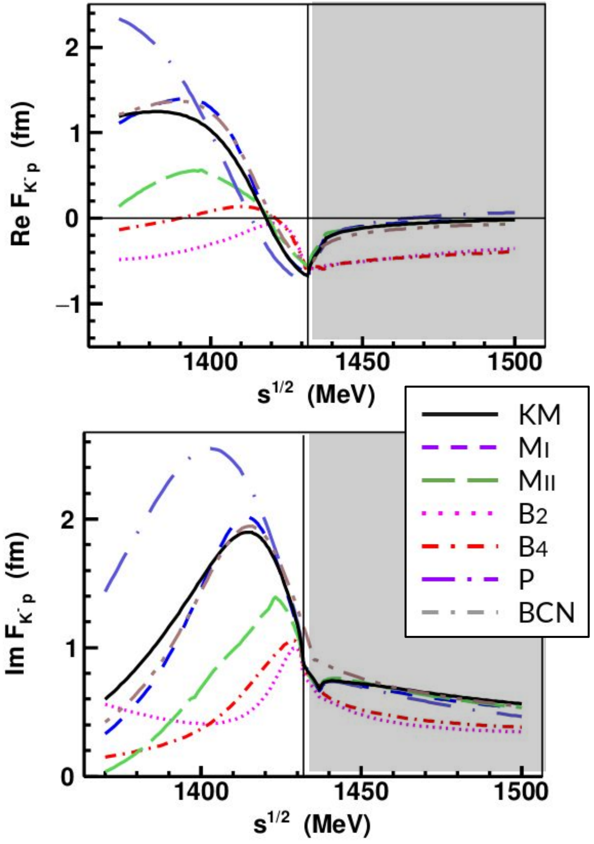

Large discrepancies in the region below threshold!

K^-p scattering amplitude with Chiral models

Kyoto-Munich (KM)
Y. Ikeda, T. Hyodo, W. Weise, Nucl. Phys. A 881 (2012) 98

Murcia (MI , MII)
Z. H. Guo, J. A. Oller, Phys. Rev. C 87 (2013) 035202

Barcelona (BCN)
A. Feijoo, V. Magas, À. Ramos, Phys. Rev. C 99 (2019) 035211

Bonn (B2 , B4)
M. Mai, U.-G. Meißner - Eur. Phys. J. A 51 (2015) 30

Prague (P)
A. C., J. Smejkal, Nucl. Phys. A 881 (2012) 115

K-p elastic and inelastic low-energy cross sections

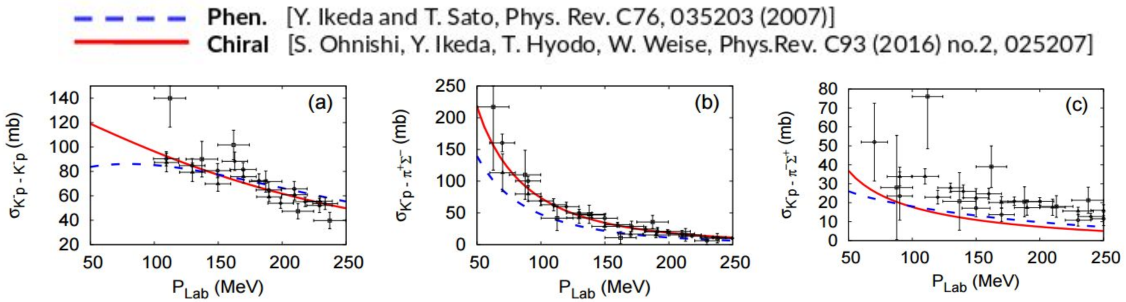

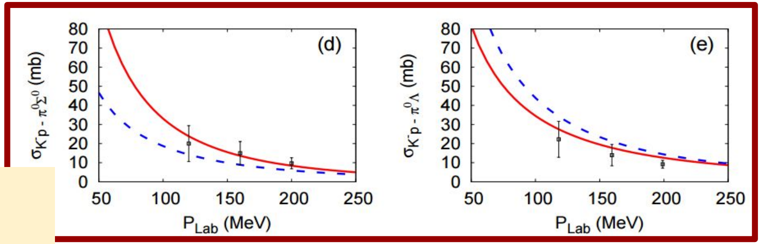

no data for $p_K < 100$ MeV/c

Experimental constraints at threshold

K^-p scattering amplitude

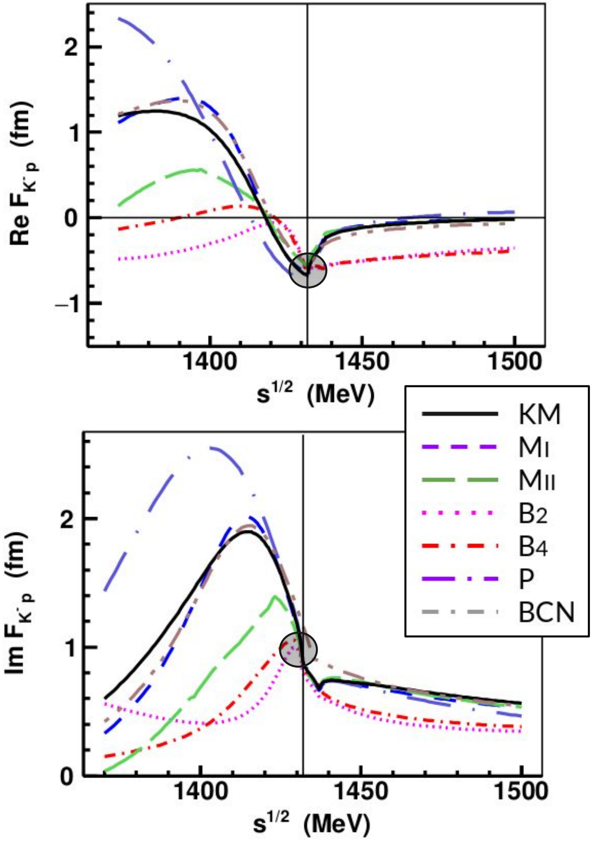

Large discrepancies in the region below threshold!

Precise SIDDHARTA measurement of kaonic hydrogen 1s level shift and width

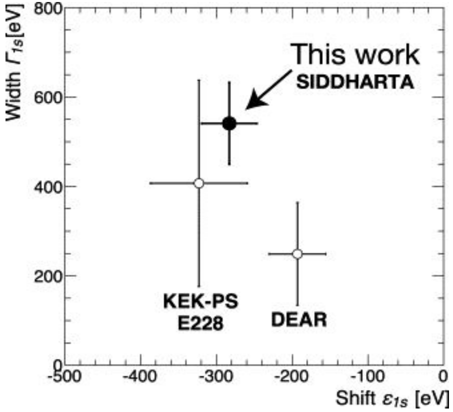

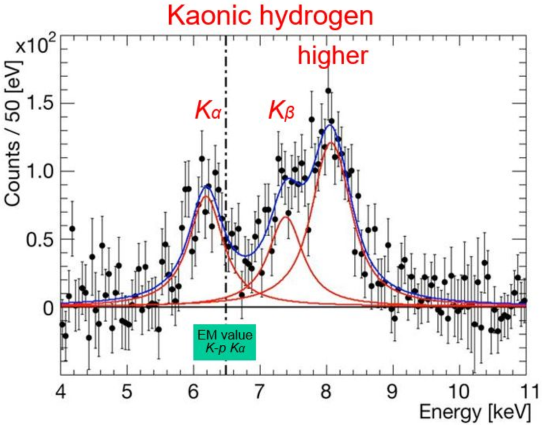

M. Bazzi et al.. 2011. (SIDDHARTA Coll.), Phys. Lett. B704, 113

$$\Delta E_N(1s) = 283 \pm 36(stat.) \pm 6(syst.)\ \text{eV}$$
$$\Gamma(1s) = 541 \pm 89(stat.) \pm 22(syst.)\ \text{eV}$$

$$\varepsilon + \frac{i\Gamma}{2} = 2\alpha^3\mu^2 a_{K^-p} = 412\,\frac{eV}{fm}\,a_{K^-p}$$

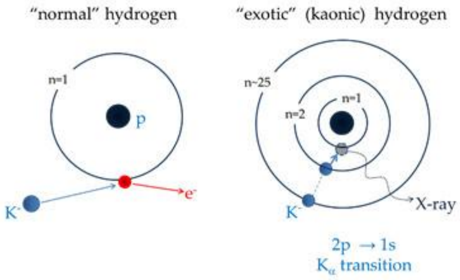

Experimental constraints below threshold

$K^{-}p$ scattering amplitude

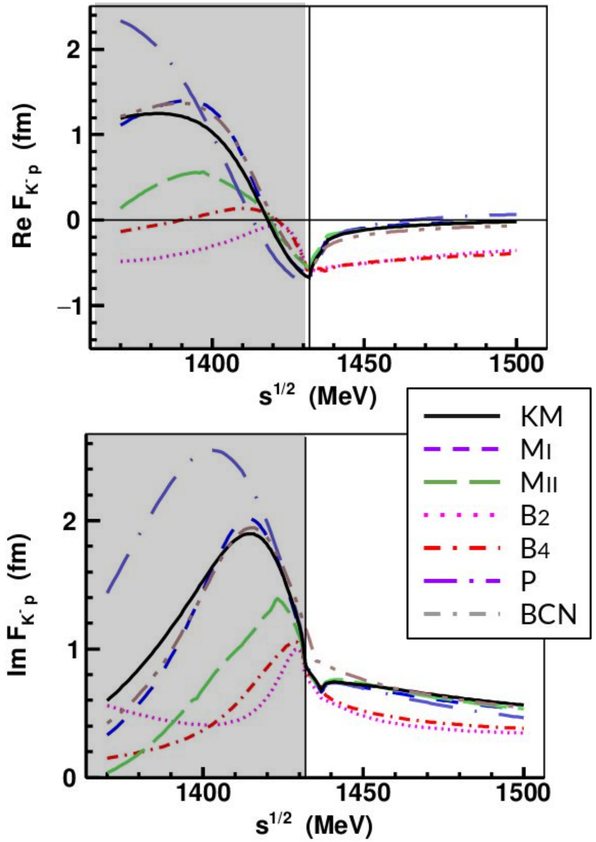

No data below threshold

NEW EXPERIMENTAL CONSTRAINTS ARE STRONGLY NEEDED!!

$\Lambda\pi^-$ analysis: K^-n non-resonant transition amplitude

THE "LINE-SHAPE" OF THE $\Lambda(1405)$ DEPENDS ON THE OBSERVED CHANNEL !!

$$\frac{d\sigma(\Sigma^-\pi^+)}{dM} \propto \frac{1}{3}|T^0|^2 + \frac{1}{2}|T^1|^2 + \frac{2}{\sqrt{6}}Re(T^0T^{1*})$$

$$\frac{d\sigma(\Sigma^+\pi^-)}{dM} \propto \frac{1}{3}|T^0|^2 + \frac{1}{2}|T^1|^2 - \frac{2}{\sqrt{6}}Re(T^0T^{1*})$$

$$\frac{d\sigma(\Sigma^0\pi^0)}{dM} \propto \frac{1}{3}|T^0|^2$$

IS DIFFERENT IN $\Sigma^+\pi^-$ VS $\Sigma^-\pi^+$

DUE TO ISOSPIN INTERFERENCE

THE CLEANEST SIGNATURE OF THE $\Lambda(1405)$ IS C
CHANNEL:

- is free from isospin interference
- is purely I = 0, no $\Sigma(1385)$ contamination.

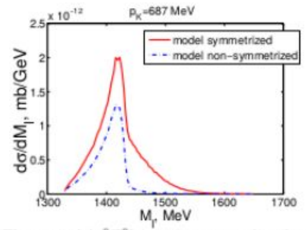

FIG. 4: Theoretical $(\pi^0\Sigma^0)$ invariant mass distribution for an initial kaon lab momenta of 687 MeV. The non-symmetrized distribution also contains the factor 1/2 in the cross section.

Phys.Rev.Lett.95:0523

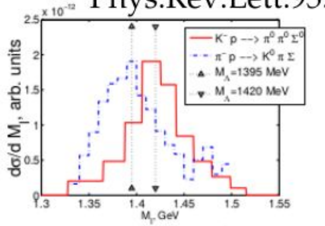

FIG. 5: Two experimental shapes of $\Lambda(1405)$ resonance. See text for more details.

Λπ⁻ analysis: K⁻n non-resonant transition amplitude

Λ(1405) case

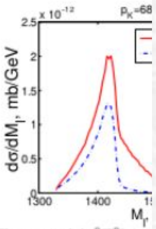

FIG. 4: Theoretical $(\pi^0\Sigma^0)$ inv
initial kaon lab momenta of 68
distribution also contains the f

Two main biases:

- the kinematical energy threshold 1412 MeV

  ($M_K + M_p$ - | BE_p |) the high pole energy region is closed,

- The shape and the amplitude of the NON-RESONANT

  Σπ production below KbarN threshold is unknown.

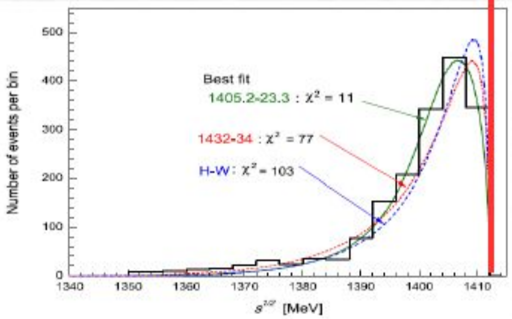

Fig. 6. Detailed differences in $M_{\Sigma\pi}$ spectra among the Hyodo–Weise prediction and the present model predictions.

An ideal experiment:

- Λ(1405) is produced in K- p absorption → mainly coupled to the high mass pole,
- Λ(1405) is observed in the $\Sigma^0\pi^0$ decay channel (pure isospin 0),
- K- is absorbed in-flight on a bound proton with p_K ~ 100 MeV, Σπ invariant mass gain of ~ 10 MeV to open an energy window to the high mass pole.
- Knowledge of the Σπ NON-RESONANT production amplitude … a choice of the resonant amplitude necessary to model simulations

K^-n scattering amplitude

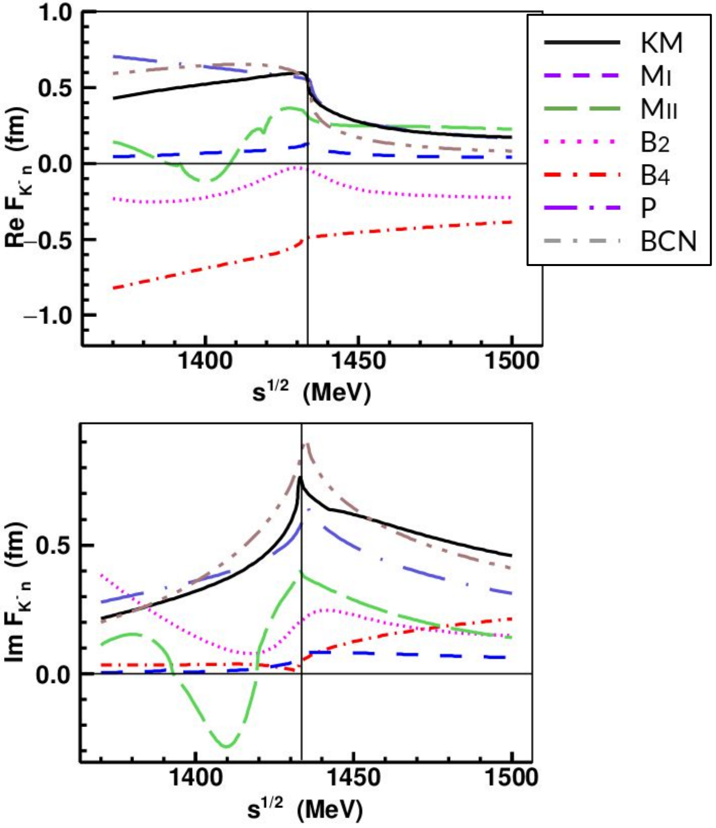

K^-n scattering amplitude with Chiral models

Large spread in I=1 channel

Experimental information is totally missing:

- **SIDDHARTA-2 → first experimental constraint at threshold**
- **AMADEUS → first experimental constraint below threshold**

AMADEUS @ DAΦNE

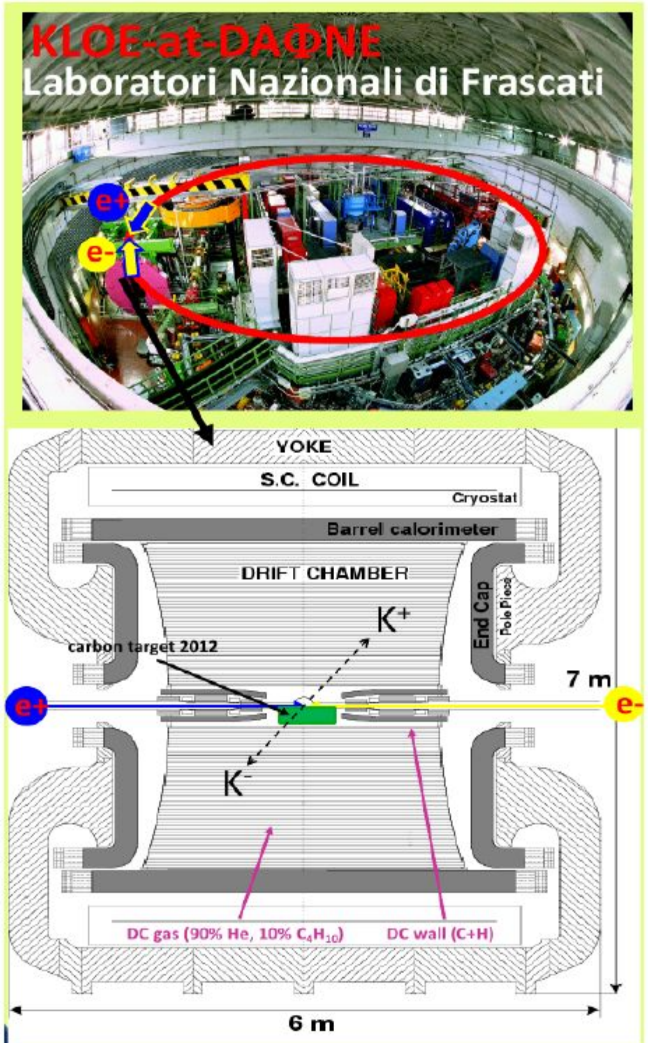

DAΦNE

- $\phi \to K^- K^+$ (49.2%), ≈1000 ϕ/s
- monochromatic **low momentum** Kaons ≈127 Mev/c
- **back to back** $K^- K^+$ topology
- **small hadronic background** due to the beam

KLOE

- Cilindrical DC with **4π geometry** & electromagnetic calormeter
- **96% acceptance**
- **high efficiency and resolution** for charged and neutral particles
- exclusive measurement of the considered

K^- absorption on light nuclei
AT REST & IN FLIGHT

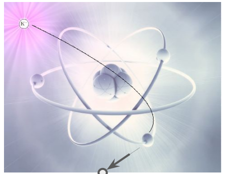

K- absorbed from atomic orbit

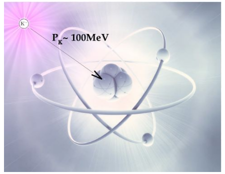

AMADEUS: KLOE 2004-2005 dataset analysis ($\mathcal{L}$ = 1.74 pb-1)

AMADEUS scientific case

- nature of Λ(1405) and K^-N amplitude below threshold

- K^- multiN absorption

- kaonic nuclear clusters

YN correlation studies
(Λp, Σ^0p, Λt)

- low-energy charged K cross section (for p=100MeV)

Particles identification

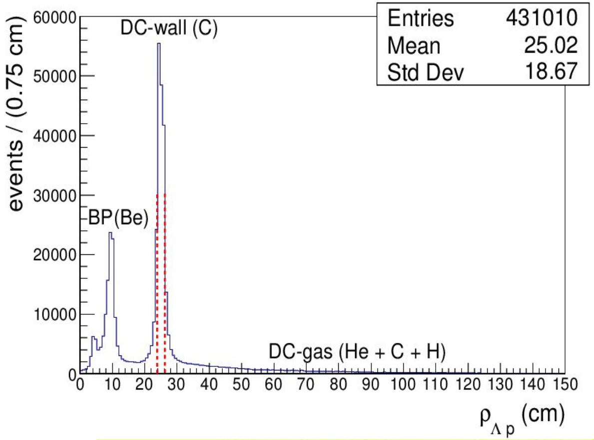

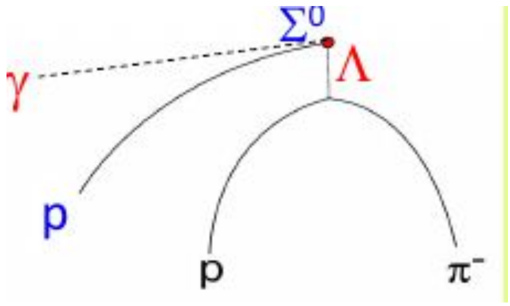

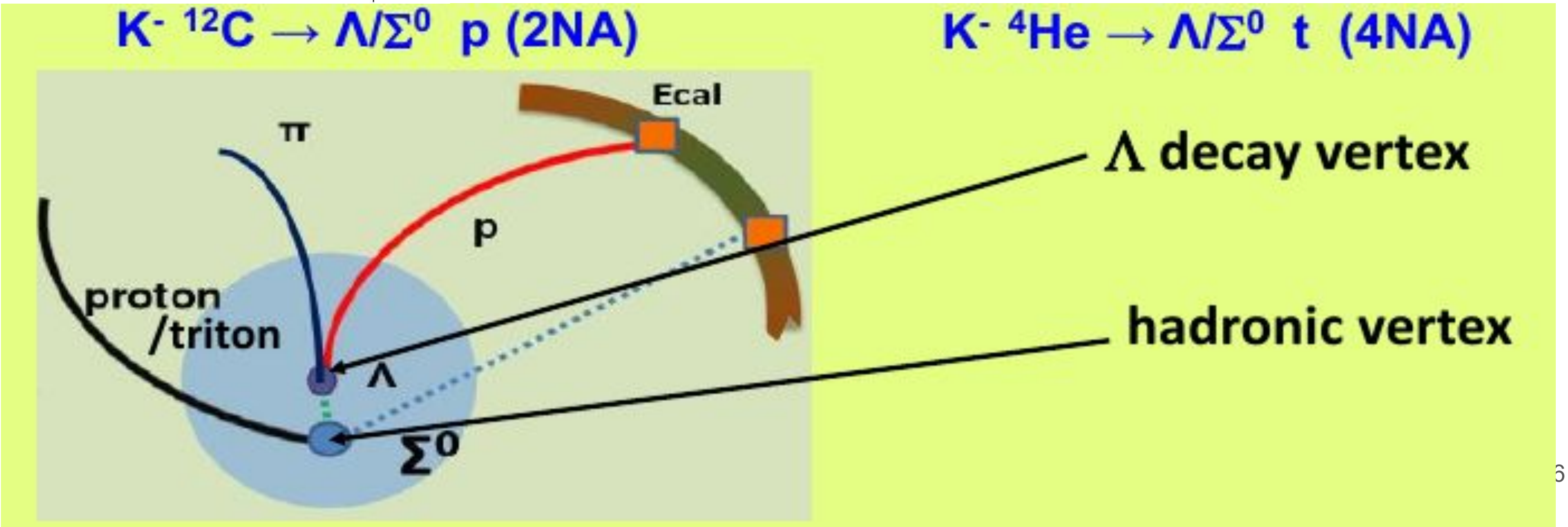

Particles identification: Λ(1116)

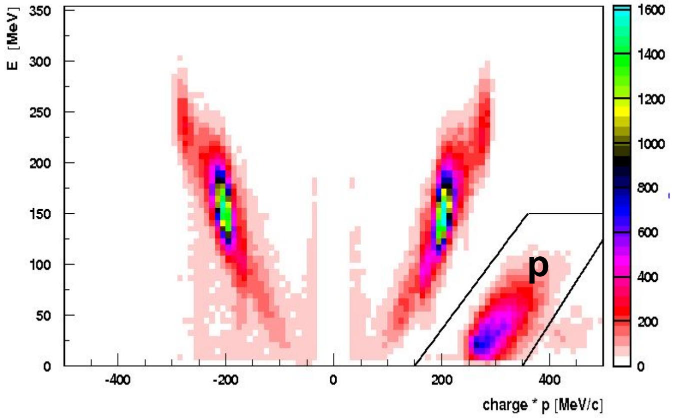

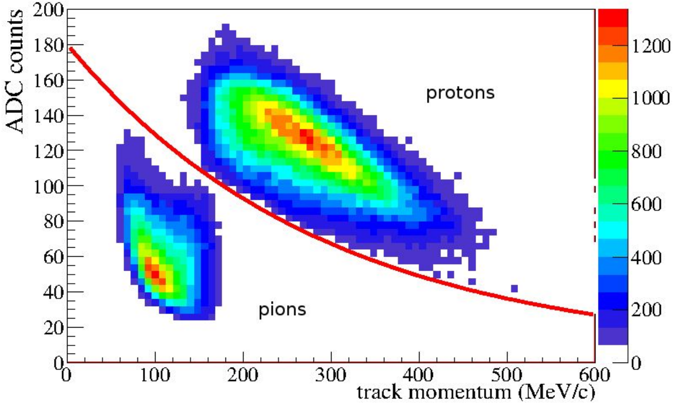

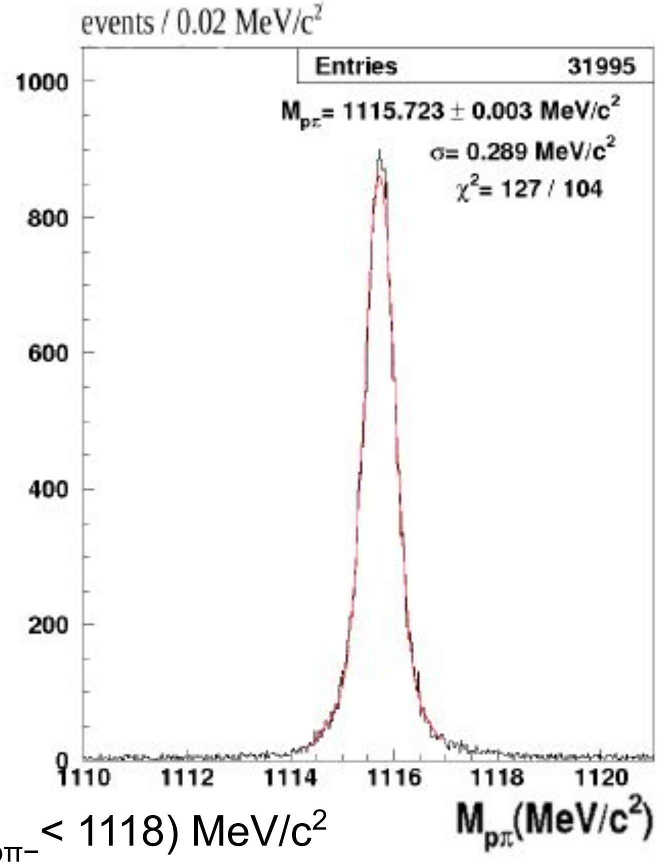

cut (1112< $M_{p\pi^-}$< 1118) MeV/c^2

$K^- \ ^{12}C \rightarrow \Lambda/\Sigma^0 \ p$ (2NA) $K^- \ ^4He \rightarrow \Lambda/\Sigma^0 \ t$ (4NA)

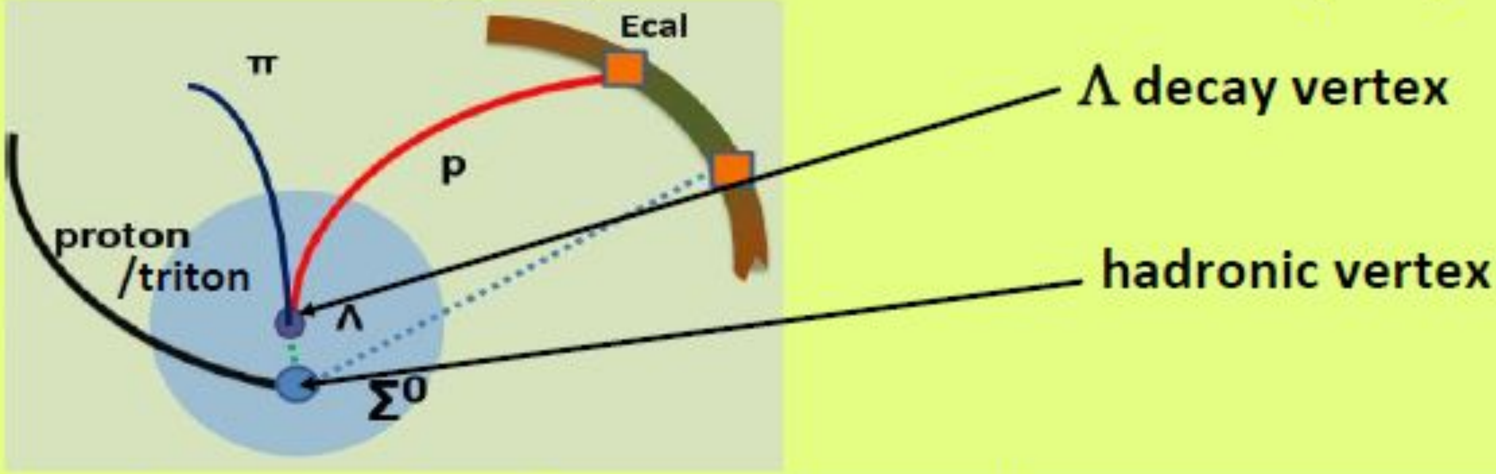

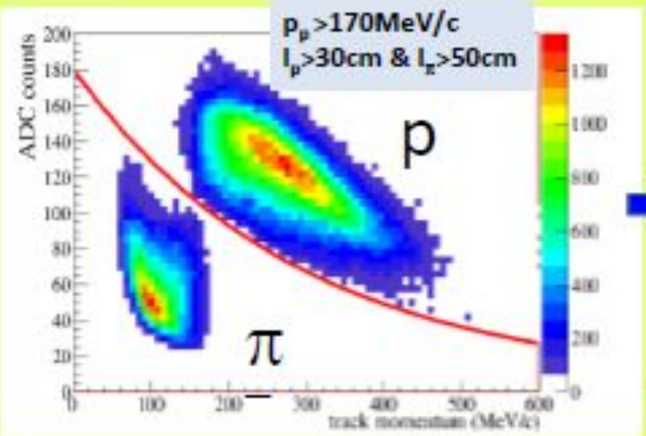

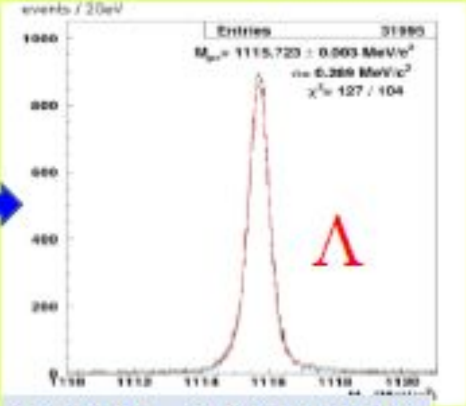

$1112 < M_{p\pi} < 1118$ MeV/c²

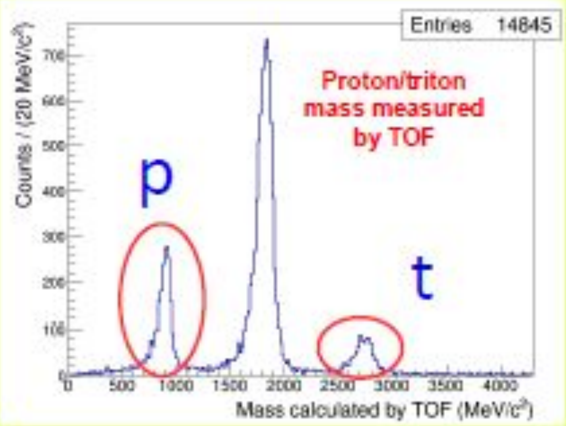

Σ^0p analysis: K^- multi-nucleon absorptions in ^{12}C

Final fit

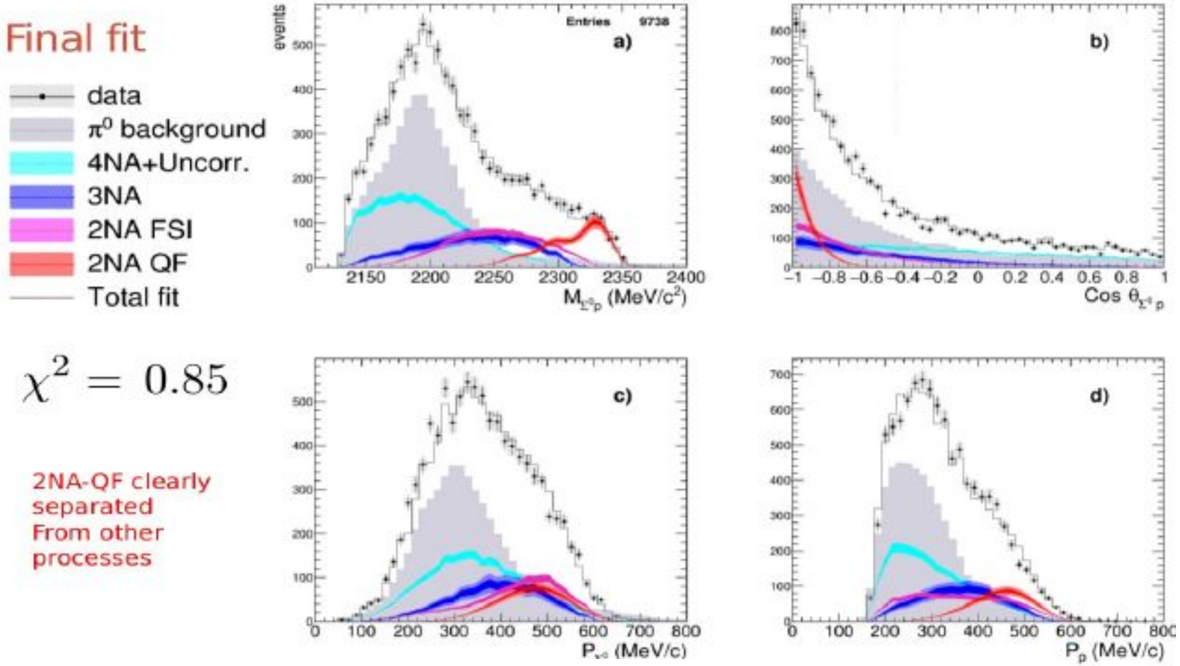

$$\chi^2 = 0.85$$

2NA-QF clearly separated From other processes

$K^-\ ^{12}C \rightarrow \Sigma^0\ p\ R \rightarrow$ **(p π^-) γ p** R

detected particles

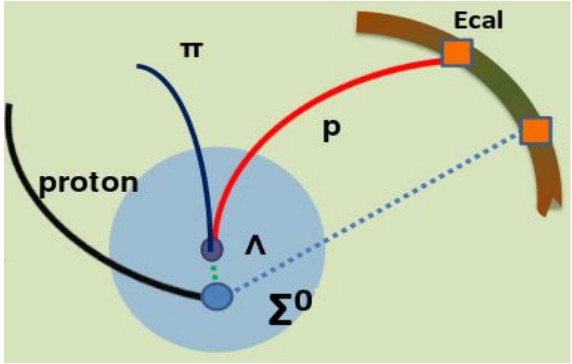

	yield / $K^-_{stop} \cdot 10^{-2}$	$\sigma_{stat} \cdot 10^{-2}$	$\sigma_{syst} \cdot 10^{-2}$
2NA-QF	0.127	$\pm$ 0.019	$^{+0.004}_{-0.008}$
2NA-FSI	0.272	$\pm$ 0.028	$^{+0.022}_{-0.023}$
Tot 2NA	0.376	$\pm$ 0.033	$^{+0.023}_{-0.032}$
3NA	0.274	$\pm$ 0.069	$^{+0.044}_{-0.021}$
Tot 3body	0.546	$\pm$ 0.074	$^{+0.048}_{-0.033}$
4NA + bkg.	0.773	$\pm$ 0.053	$^{+0.025}_{-0.076}$

O. Vazquez Doce, et. al., Phys. Lett. B758, 134 (2016)

The controversial nature of the Λ(1405)

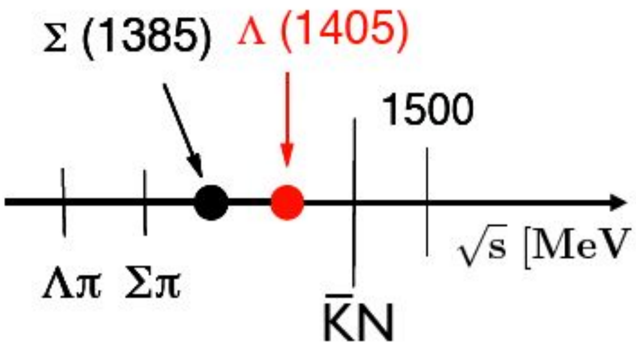

The Λ(1405) state does not fit with the simple three quarks model (*uds*) and it is commonly accepted that **it is, at least partially, a K̄N bound state**.

- **Chiral SU(3) coupled channel dynamics:** the state is given by the superpositions of **two poles of the K̄N scattering amplitude**.

  M = 1425 MeV → **mainly coupled to the K̄N channel**

  M = 1380 MeV → **mainly coupled to the Σπ channel**

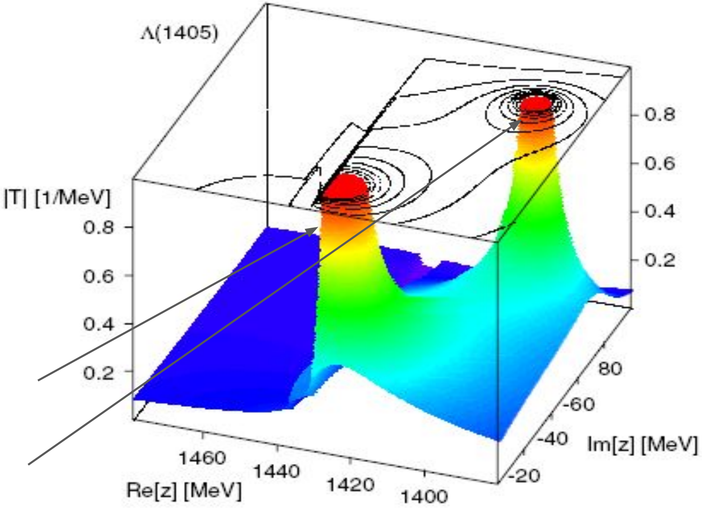

- **Phenomenological potentials models:** the **Λ(1405) is a pure K̄N bound state** with mass M=1405 MeV, binding energy BE = 27 MeV and width Γ=50 MeV.

Possible existence of kaonic bound states

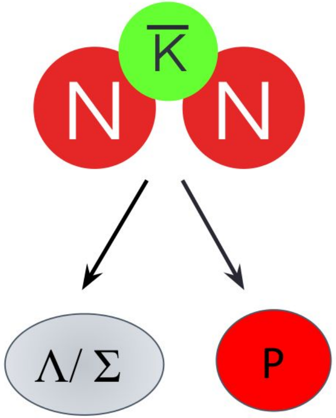

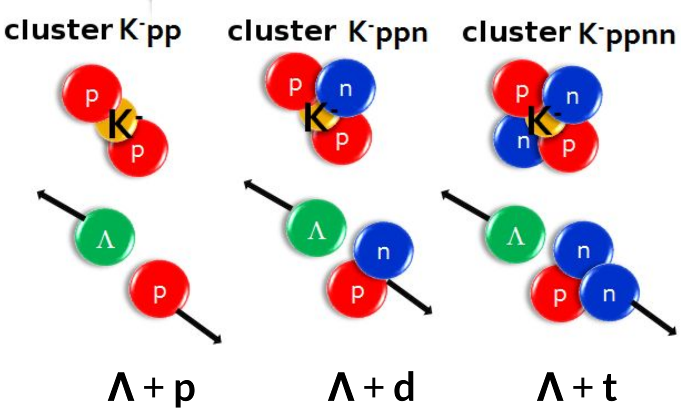

Wycech (1986) - Akaishi & Yamazaki (2002)

Predicted in the **$\bar{K}$N interaction in the I=0** channel due to the strong interaction (deeply bound kaonic nuclear states)

largely compressed due to the strong attraction

Kaonic Nuclei	Binding Energy [MeV]	Width [MeV]	Central Density
K-p	27	40	$3.5\rho_0$
K-pp	48	61	$3.1\rho_0$
K-ppp	97	13	$9.2\rho_0$
K-ppn	118	21	$8.8\rho_0$

ρ_0 =0.17 fm^{-3}

EoS of the Neutron Stars

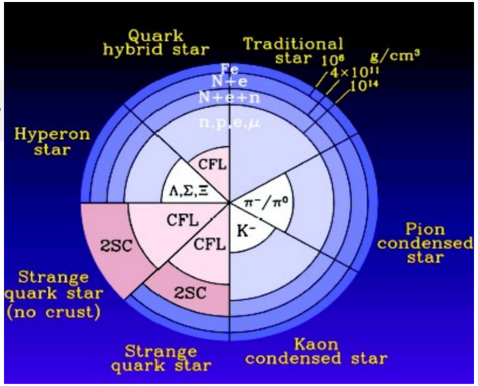

The central densities are expected to be large enough to activate the strangeness production:

$$p + e^- \rightarrow n + \nu_e$$
$$n \rightarrow p + K^-$$

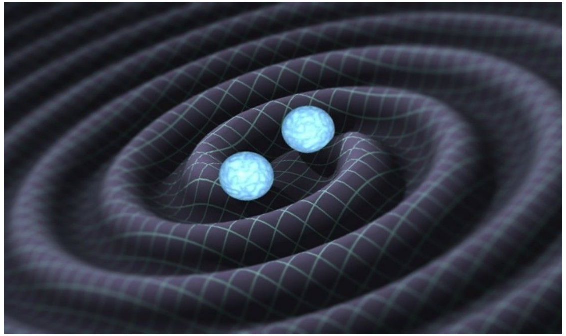

Possible existence of kaonic bound states

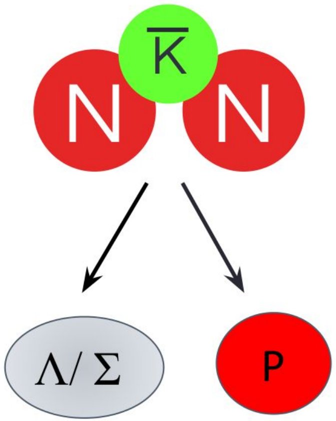

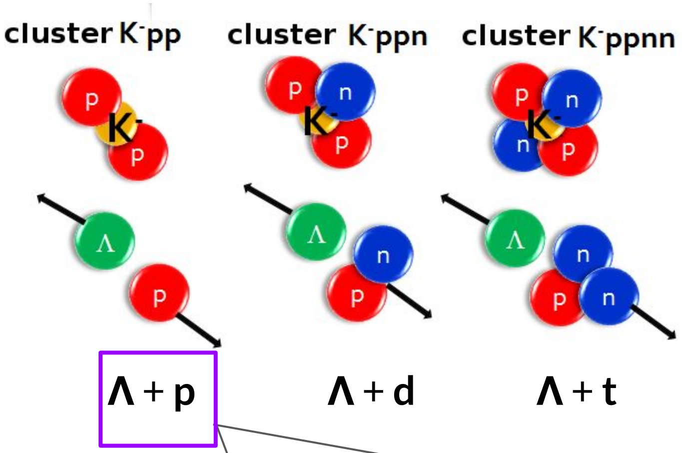

Wycech (1986) - Akaishi & Yamazaki (2002)

Predicted in the **K̄N interaction in the I=0** channel due to the strong interaction

Essential impact on the EoS of Neutron Stars

gravitational waves signal emitted by binary system of Neutron Stars

Theory

Chiral models	BE [MeV]	Γ [MeV]	Reference
Dote, Hyodo, Weise	17 - 23	40 - 70	Phys. Rev. C 79 (2009) 014003
Barnea, Gal, Liverts	16	41	Phys. Lett. B 712 (2012) 132
Ikeda, Kamano, Sato	9 - 16	34 - 46	Prog. Theor. Phys. (2010) 124 (3)
Bicudo	14.2 - 53	13.8 - 28.3	Phys. Rev. D 76 (2007) 031502
Bayar, Oset	15 - 30	75 - 80	Nucl. Phys. A 914 (2013) 349
Dote, Inoue, Myo	21.2 - 32.2	9 - 31.7	Prog. Theor. Exp. Phys. 2015 (2015) 043D02
Sekihara, Oset, Ramos	16	72	Prog. Theor. Exp. Phys. 2016 (2016) 123D03
Phen. approach	**BE [MeV]**	**Γ [MeV]**	**Reference**
Akaishi, Yamazaki	48	61	Phys. Rev. C 65 (2002) 044005
Ikeda, Sato	60 - 95	45 - 90	Phys. Rev. C 76 (2007) 035203
Shevchenko, Gal, Mares	55 - 70	90 - 110	Phys. Rev. Lett. 98 (2007) 082301
Revai, Shevchenko	32	49	Phys. Rev. C 90 no. 3 (2014) 034004
Maeda, Akaishi, Yamazaki	51.5	61	Proc. Jpn. Acad. B 89 (2013) 418
Wycech, Green	40 - 80	40 - 85	Phys. Rev. C 79 (2009) 014001

Experiments

Experiment	BE [MeV]	Γ [MeV]	Reference
FINUDA	115^{+6}_{-5}(stat.)$^{+3}_{-4}$(syst.)	67^{+14}_{-11}(stat.)$^{+2}_{-3}$(syst.)	PRL 94 (2005), 212303
OBELIX	160.9±4.9	<24.4±8.0	NPA 789 (2007), 222
E549	-	-	MPLA 23 (2008), 2520
DISTO	103±3(stat.)±5(syst.)	118±8(stat.)±10(syst.)	PRL 104 (2010), 132502
LEPS/SPring-8	Upper limit		PLB 728 (2014), 616
HADES	Upper limit		PLB 742 (2015), 242
E27	95^{+18}_{-17}(stat.)$^{+30}_{-21}$(syst.)	162^{+87}_{-45}(stat.)$^{+66}_{-78}$(syst.)	PTEP (2015), 021D01
AMADEUS	Upper limit		PLB 758 (2016), 134
E15 1st run	15^{+6}_{-8}(stat.)±12(syst.)	110^{+19}_{-17}(stat.)±27(syst.)	PTEP (2016), 051D01
E15 2nd run	47±3(stat.)$^{+3}_{-6}$(syst.)	115±7(stat.)$^{+10}_{-20}$(syst.)	PLB 789 (2019), 612

Possible existence of kaonic bound states

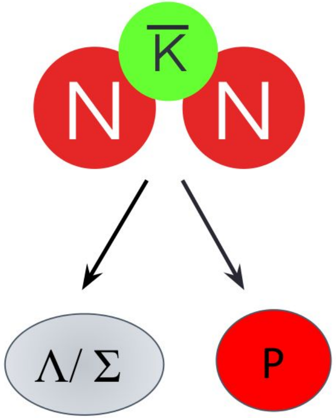

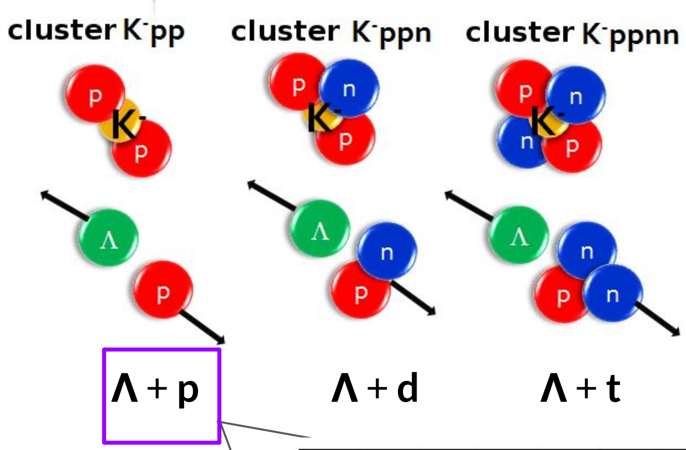

Wycech (1986) - Akaishi & Yamazaki (2002)

Predicted in the **$\overline{K}$N interaction in the I=0** channel due to the strong interaction

Essential impact on the EoS of Neutron Stars

gravitational waves signal emitted by binary system of Neutron Stars

Theory

Chiral models	BE [MeV]	Γ [MeV]	
Dote, Hyodo, Weise	17 - 23	40 - 70	Phys
Barnea, Gal, Liverts	16	41	Phy
Ikeda, Kamano, Sato	9 - 16	34 - 46	Prog.
Bicudo	14.2 - 53	13.8 - 28.3	Phys
Bayar, Oset	15 - 30	75 - 80	Nuc
Dote, Inoue, Myo	2[illegible]		Theo
Sekihara, Oset, Ramos			Theo
Phen. approach	**BE**		
Akaishi, Yamazaki	48	61	Phys
Ikeda, Sato	60 - 95	[illegible]90	Phys
Shevchenko, Gal, Mares	55 - 70	9[illegible] 110	Phys.
Revai, Shevchenko	32	[illegible]9	Phys. I
Maeda, Akai[illegible]			
Wycec[illegible]			

Takumi Yamaga
Friday, 10:30

E15 → first clear evidence in K⁻ induced reactions
Phys. Lett. B 789 (2019) 620-625

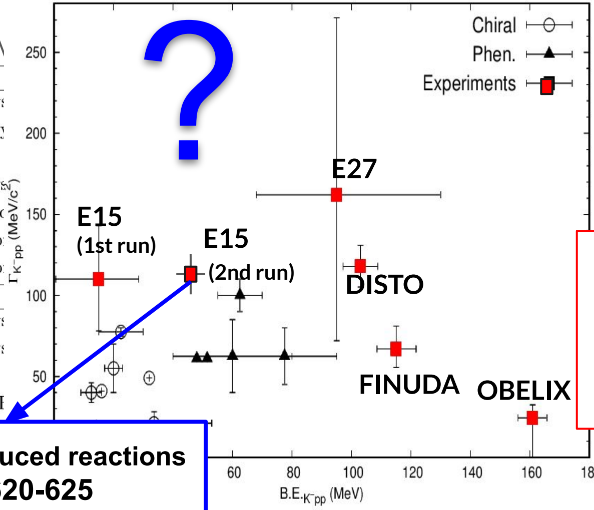

Experiments

BE [MeV]	Γ [MeV]	Reference
[illegible]5^{+6}_{-5}(stat.)$^{+3}_{-4}$(syst.)	67^{+14}_{-11}(stat.)$^{+2}_{-3}$(syst.)	PRL 94 (2005), 212303
160.9±4.9	<24.4±8.0	NPA 789 (2007), 222
-	-	MPLA 23 (2008), 2520
[illegible]$_{-8}$(stat.)±12(syst.)	$110^{+[illegible]}_{-17}$(stat.)±27(syst.)	PTEP (2016), 051D01
[illegible]±3(stat.)$^{+3}_{-6}$(syst.)	115±7(stat.)$^{+10}_{-20}$(syst.)	PLB 789 (2019), 612

FINUDA, E549, E15, AMADEUS: K⁻ induced reactions
DISTO, HADES: p-p collisions
OBELIX: anti-p annihilations
E27: π induced reactions
LEPS/SPring-8: photoproduction

$\Lambda\pi^-$ analysis: K^-n non-resonant transition amplitude

$\Lambda(1405)$ case

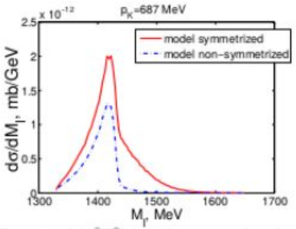

FIG. 4: Theoretical $(\pi^0\Sigma^0)$ invariant mass distribution for an initial kaon lab momenta of 687 MeV. The non-symmetrized distribution also contains the factor 1/2 in the cross section.

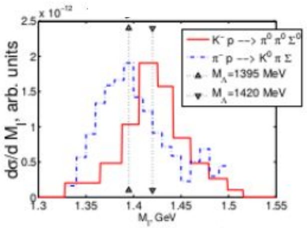

FIG. 5: Two experimental shapes of $\Lambda(1405)$ resonance. See text for more details.

Goal: how much comes from resonance in $K^-N \rightarrow Y\pi$

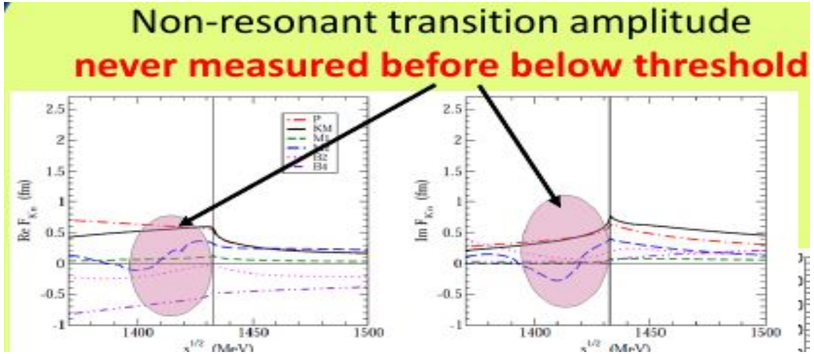

J. Hrtankova, J. Mares, Phys. Rev. C96, 015205 (2017)
A. Cieply et al, Nycl. Phys. A 954, 17 (2016)

IN FLIGHT K^- ^{12}C opens window between 1416 MeV and KN threshold

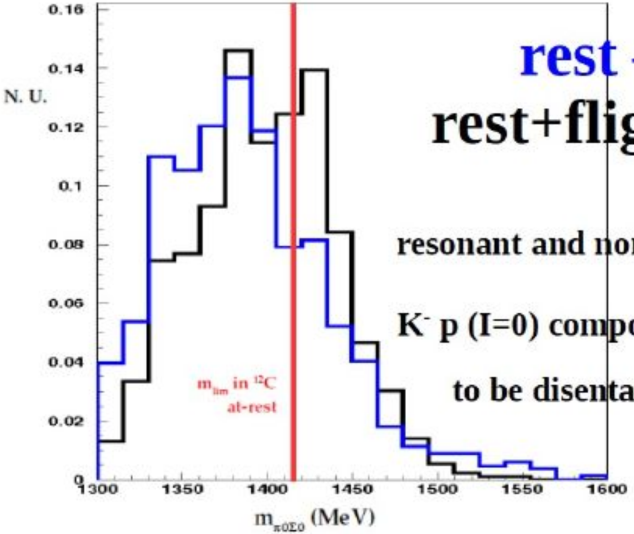

rest –
rest+flight –

resonant and non-resonant

K^- p (I=0) components are

to be disentangled

K^-"n" $\rightarrow$ $\Lambda\pi^-$ direct formation in ^{4}He

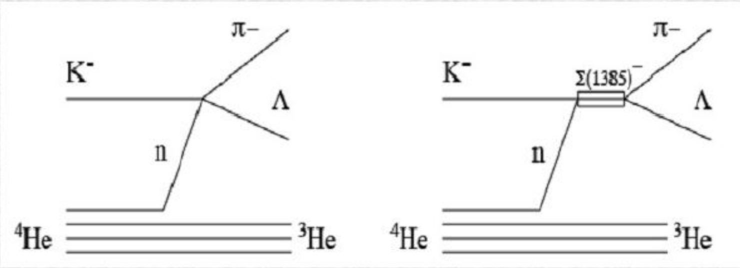

$$|f^{N\text{-}R}_{\Lambda\pi}(I=1)| \Rightarrow |f^{N\text{-}R}_{\Sigma\pi}(I=0)|$$

$K^- \, {}^4He \to \Lambda p^- \, {}^3He$ resonant and non-resonant processes

K. P., S. Wycech and C. Curceanu, Nucl. Phys. A954 (2016) 75-93
R. Del Grande, K. P., S. Wycech, Acta Phys. Pol. B 48 (2017) 1881

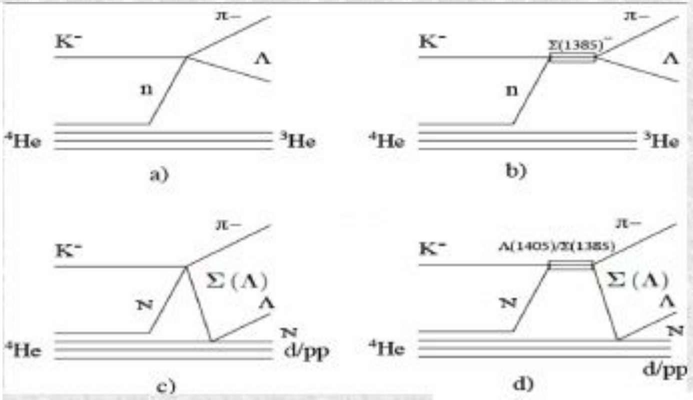

Simulations for resonant and non-resonant processes performed based on calculations for both S-state and P-state K- capture AT REST and IN FLIGHT

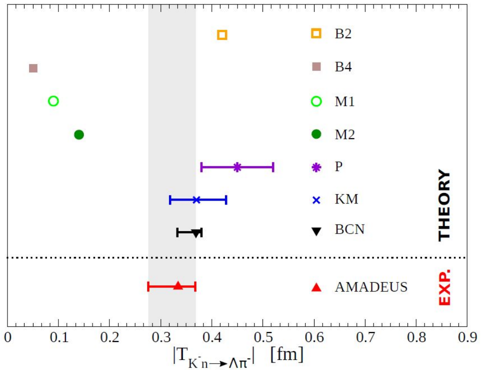

K. Piscicchia, et. al., Phys. Lett. B782, 339 (2018)

Simultaneous fit : $(p_{\Lambda\pi-}$ - $m_{\Lambda\pi-}$ - $\cos(\theta_{\Lambda\pi-})$)

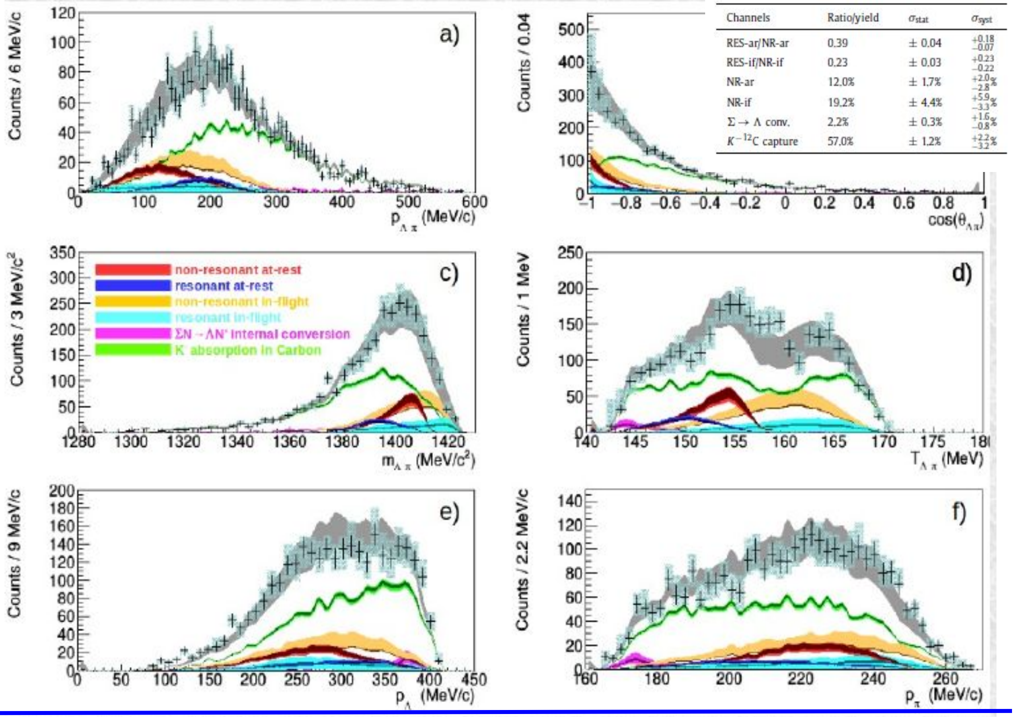

Channels	Ratio/yield	σ_{stat}	σ_{syst}
RES-ar/NR-ar	0.39	± 0.04	$^{+0.18}_{-0.07}$
RES-if/NR-if	0.23	± 0.03	$^{+0.23}_{-0.22}$
NR-ar	12.0%	± 1.7%	$^{+2.0}_{-2.8}$%
NR-if	19.2%	± 4.4%	$^{+5.9}_{-3.3}$%
$\Sigma \to \Lambda$ conv.	2.2%	± 0.3%	$^{+1.6}_{-0.8}$%
$K^- {}^{12}C$ capture	57.0%	± 1.2%	$^{+2.2}_{-3.2}$%

From the well known Σ* transition probability:

$$\frac{NR-ar}{RES-ar} = \frac{\int_0^{pmax} P_{ar}^{nr}(p_{\Lambda\pi})\, dp_{\Lambda\pi}}{\int_0^{pmax} P_{ar}^{res}(p_{\Lambda\pi})\, dp_{\Lambda\pi}} =$$

$$= |f_{ar}^s|^2 \cdot 8,94 \cdot 10^5 \mathrm{MeV}^2$$

$$|f_{ar}^{nr}| = |A_{K-n\to\Lambda\pi-}| = (0.334 \pm 0.018\,\mathrm{stat}^{+0.034}_{-0.058}\mathrm{syst})\ \mathrm{fm}$$

1) extract the amplitude for each model .. $A_{K\text{-}n} = (\mathrm{Re}F^2_{K\text{-}n} + \mathrm{Im}F^2_{K\text{-}n})^{1/2}$
2) scale the amplitudes for the K^-n couplings to the $\Sigma^-\pi^0$ and $\Sigma^0\pi^-$ channels:

$$\frac{Prob_{K^-n\to\Lambda\pi^-}}{Prob_{K^-n\to\Sigma^-\pi^0}} = \frac{Ph_{K^-n\to\Lambda\pi^-}}{c_1 Ph_{K^-n\to\Sigma^-\pi^0}}$$

Isospin (I, I_z) = = (1 , -1) component

Phase spaces ratios

$$\frac{Prob_{K^-n\to\Lambda\pi^-}}{Prob_{K^-n\to\Sigma^0\pi^-}} = \frac{Ph_{K^-n\to\Lambda\pi^-}}{c_2 Ph_{K^-n\to\Sigma^0\pi^-}}$$

Λt analysis: Cross section and BR for 4NA in $K^{-}\,{}^{4}He \rightarrow \Lambda t$ process

Previous data:

- in ^{4}**He:** bubble chamber experiment

/M. Roosen, J. H. Wickens, Il Nuovo Cimento 66, 101 (1981)/

only **3 events** compatibile with Λt kinematics found

$BR(K^{-}\,{}^{4}He \rightarrow \Lambda t) = (3 \pm 2) \times 10^{-4} / K_{stop}$ → **global, no 4NA**

- in **solid targets:** ^{6,7}**Li,** ^{9}**Be** (FINUDA)

/Phys. Lett. B, 229 (2008)/

40 events, only **back-to-back data**

Λt emission yield → $10^{-3} - 10^{-4} / K^{-}_{stop}$ → **global, no 4NA**

Λt analysis: Cross section and BR for 4NA in $K^- \, ^4He \rightarrow \Lambda t$ process

Previous data:

- in ^{4}**He:** bubble chamber experiment

/M. Roosen, J. H. Wickens, Il Nuovo Cimento 66, 101 (1981)/

only **3 events** compatibile with Λt kinematics found

BR$(K^- \, ^4He \rightarrow \Lambda t)$ **=** $(3 \pm 2) \times 10^{-4} / K_{stop}$ → **global, no 4NA**

- in **solid targets:** ^{6,7}**Li,** ^{9}**Be** (FINUDA)

/Phys. Lett. B, 229 (2008)/

40 events, only **back-to-back data**

Λt emission yield $\rightarrow 10^{-3} - 10^{-4} / K^-_{stop}$ → **global, no 4NA**

AMADEUS analysis

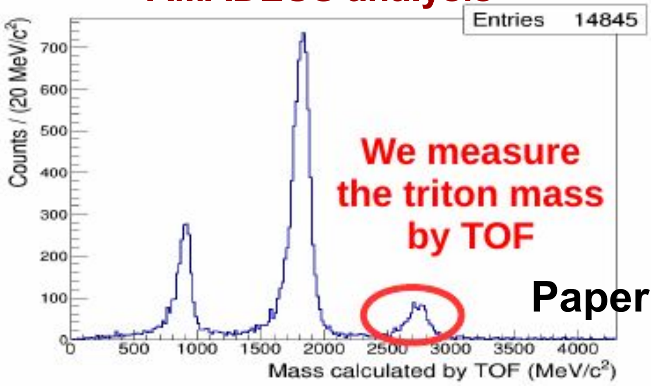

Paper in preparation

Final fit

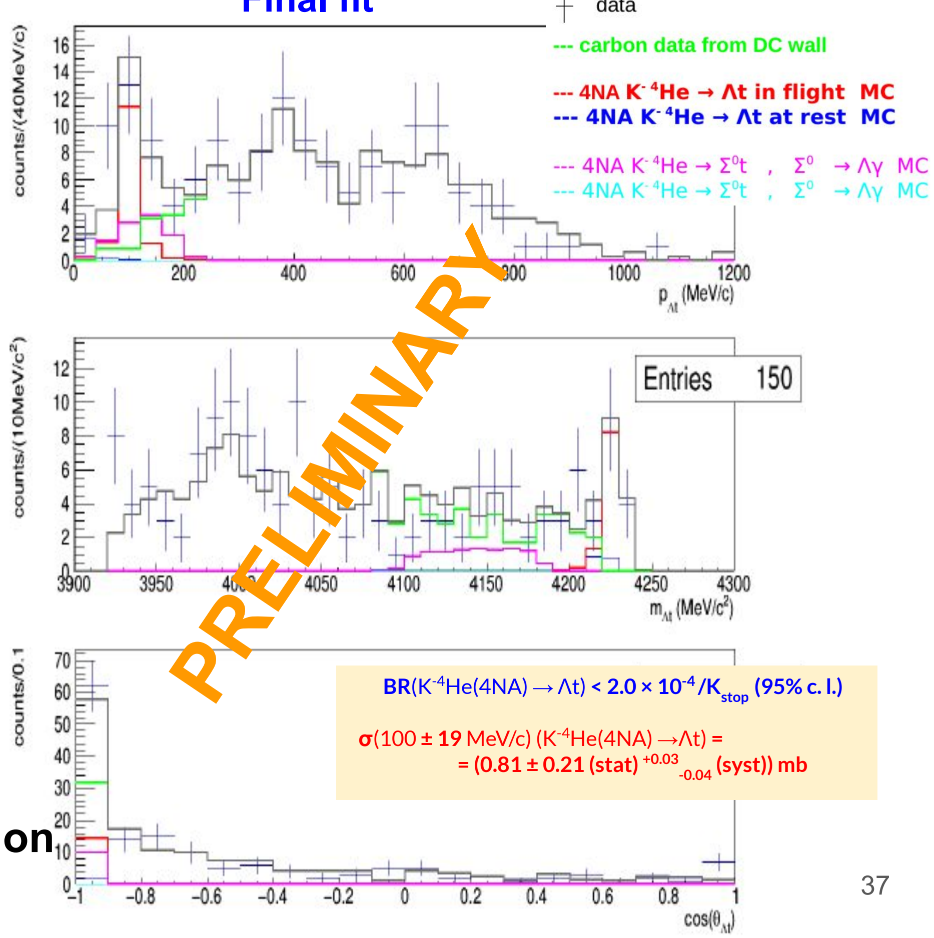

BR$(K^- \, ^4He(4NA) \rightarrow \Lambda t)$ **<** $2.0 \times 10^{-4} / K_{stop}$ **(95% c. l.)**

$\sigma(100 \pm 19$ MeV/c$)$ $(K^- \, ^4He(4NA) \rightarrow \Lambda t) =$
$= (0.81 \pm 0.21 \text{ (stat)} \, ^{+0.03}_{-0.04} \text{ (syst)})$ mb

Λt analysis: Cross section and BR for 4NA in $K^{-}\,{}^{12}C \rightarrow \Lambda t$ process

Previous data:

- in ^{4}**He:** bubble chamber experiment

/M. Roosen, J. H. Wickens, Il Nuovo Cimento 66, 101 (1981)/

only **3 events** compatibile with Λt kinematics found

BR$(K^{-}\,{}^{4}He \rightarrow \Lambda t) = (3 \pm 2) \times 10^{-4} / K_{stop}$ → **global, no 4NA**

- in **solid targets:** ^{6,7}**Li,** ^{9}**Be** (FINUDA)

/Phys. Lett. B, 229 (2008)/

40 events, only **back-to-back data**

Λt emission yield → $10^{-3} - 10^{-4} / K^{-}_{stop}$ → **global, no 4NA**

AMADEUS analysis

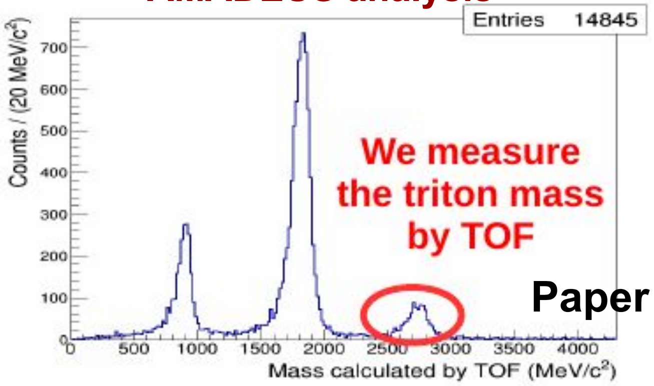

Paper in preparation

Final fit

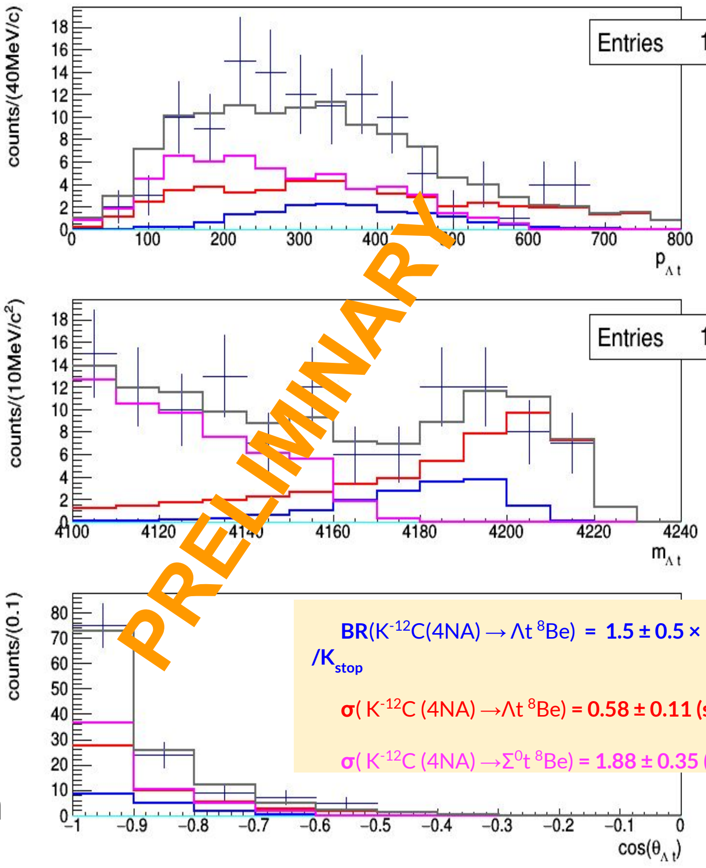

$BR(K^{-}\,{}^{12}C(4NA) \rightarrow \Lambda t\,{}^{8}Be) = 1.5 \pm 0.5 \times 10^{-4}$ (stat) $/K_{stop}$

$\sigma(K^{-}\,{}^{12}C\,(4NA) \rightarrow \Lambda t\,{}^{8}Be) = 0.58 \pm 0.11$ (stat) mb

$\sigma(K^{-}\,{}^{12}C\,(4NA) \rightarrow \Sigma^{0} t\,{}^{8}Be) = 1.88 \pm 0.35$ (stat) mb

Lambda-deuteron final state K- absorptions in 4He

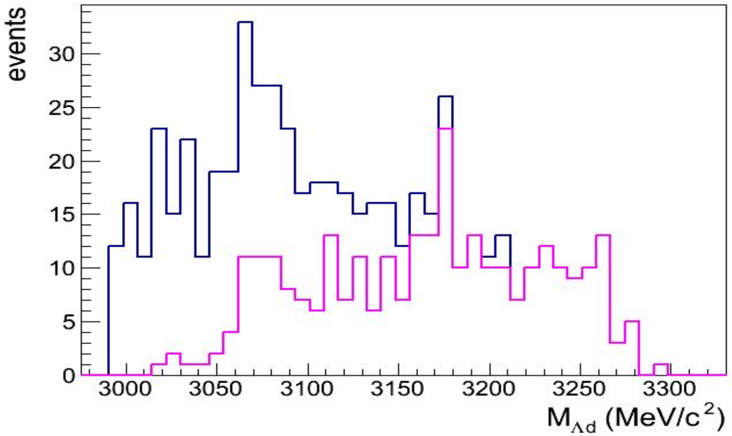

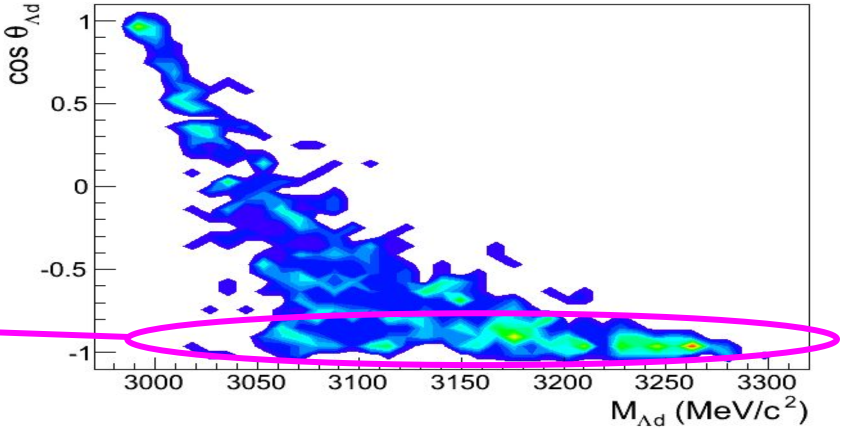

572 **Λd** events in the DC gas

Structures at high mass clearly correlated with back-to-back events